TRANSPORT OF A BACTERIAL AEROSOL IN TURBULENT MIXING REGIONS

Thesis for the Degree of Ph. D.

MICHIGAN STATE UNIVERSITY

Dennis Ray Heldman

1965

ABSTRACT

TRANSPORT OF A BACTERIAL AEROSOL IN
TURBULENT MIXING REGIONS

by Dennis Ray Heldman

The knowledge of transport mechanisms of bacterial aerosols is of primary importance when analyzing airborne contamination control methods for food processing and packaging operations. This investigation was conducted to determine the transport characteristics of a bacterial aerosol under conditions simulating two adjacent rooms with different aerosol concentrations. The experimental investigation involved determination and description of transfer coefficients for transport of an aerosol through an opening in a partition between two 64 ft^3 compartments with different uniform aerosol concentrations. Theoretical description and analysis of experimental data involved the use of a mixing region model, which described turbulent dispersion of aerosol through the opening and entrainment in the low concentration compartment.

Air velocity fluctuations were detected by a hot wire anemometer and recorded for several locations and flow conditions. Information on turbulent energy, eddy diffusivities and dispersion of the aerosol in the mixing region was

obtained by means of a statistical analysis of the air velocity records.

Experimental data were collected for equal air flow rates from 20 to 60 ft^3/min through both compartments of the aerosol chamber. In addition, tests were conducted with air flow rate gradients as high as 40 ft^3/min in the same direction or opposite the concentration gradient. Transfer coefficients and turbulent energy increased significantly as air flow rate increased from 20 to 40 ft^3/min, whereas the intensity of turbulence was relatively constant over the entire range investigated. For aerosol flow rates above 30 ft^3/min, transfer coefficients were maximum when air flow rates through both compartments were equal.

The area of the opening between the two compartments was varied by changing the vertical height to 3, 6, and 9 in. Decreasing transfer coefficients with increasing vertical height of opening were related to the shape of the mixing region profiles.

The partition width at the initial point of mixing influenced the transfer coefficients slightly. An increase in transfer coefficient occurred as the width was increased from 0.0625 to 0.3125 in., but the coefficient decreased as the width was increased to 0.5625 in. Slight increases in turbulence due to increased partition width and a reduction in mixing region width were factors involved in the explanation of this relationship.

Dennis Ray Heldman

The influence of temperature gradients on transport characteristics was determined by heating the air in one compartment of the aerosol chamber. Transfer coefficients increased consistently as the temperature gradient was increased from -14° to +12.5°F

A dimensionless relationship was derived, based on the turbulent mixing region model, and used to present all data obtained in the investigation.

Approved Carl W. Hall
Major Professor
and Department Chairman

Nov. 29, 1965
Date

TRANSPORT OF A BACTERIAL AEROSOL IN TURBULENT MIXING REGIONS

By

Dennis Ray Heldman

A THESIS

Submitted to
Michigan State University
in partial fulfillment of the requirements
for the degree of

DOCTOR OF PHILOSOPHY

Department of Agricultural Engineering

1965

ACKNOWLEDGMENTS

The guidance and leadership of Dr. C. W. Hall, chairman of the Agricultural Engineering Department, is gratefully acknowledged. The inspiration provided throughout this portion of my graduate program and during the course of this investigation has made it a pleasing and rewarding experience.

Sincere appreciation is extended to Dr. T. I. Hedrick (Food Science) for supplying facilities required for conducting experiments and for providing advice and suggestions whenever requested.

Additional acknowledgment is offered to Dr. K. L. Schulze (Sanitary Engineering) and Dr. F. H. Buelow (Agricultural Engineering) for serving as guidance committee members and providing advice whenever needed.

The unfailing support and encouragement provided by my wife, Joyce, has supplied inspiration needed throughout my undergraduate and graduate education.

To:

Joyce, Cynthia and Candace
Mr. and Mrs. M. L. Heldman
Mr. and Mrs. H. S. Anspach

TABLE OF CONTENTS

Page

LIST OF TABLES

Table | Page

LIST OF FIGURES

Figure Page

Figure | Page

LIST OF APPENDICES

NOMENCLATURE

b = apparent width of aerosol mixing region defined by equation (3.36), in.

b_o = partition width at initial point of mixing, in.

C = bacterial aerosol concentration, No./ft.^{3}

C_o = bacterial aerosol concentration at time equal to zero, No./ft.^{3}

D_a = apparent eddy diffusivity presented in equation (3.3), in^2/min.

D_t = specific eddy diffusivity defined by equation (3.32), in^2/min.

f = air flow rate, ft^3/min.

f_o = air flow rate with equal flow in both compartments of aerosol chamber, ft^3/min.

$f(\beta)$ = integral of complementary error function defined in equation (3.47), in.

H = vertical height of opening between compartments of aerosol chamber, in.

H' = vertical height of aerosol chamber.

ℓ_1 = length scale of turbulence defined in equation (3.34), in.

K = death rate constant of bacterial aerosol, 1/min.

K' = experimental constant in equation (3.42).

k_c = turbulent transfer coefficient, No./ft^2,min (No./ft^3).

N_A = mass flux of bacterial aerosol, No./min.

$R(\xi)$ = autocorrelation coefficient defined in equation (3.21)

t = aerosol dispersion time, min.

T = time required for $R(\xi)$ to approach zero, sec

u = air velocity parallel to x-axis, ft/min.

$\overline{u'^2}$ = turbulent energy factor for longitudinal direction, ft^2/min^2

v = air velocity parallel to y-axis, ft/min.

$\overline{v'^2}$ = turbulent energy factor for transverse direction, ft^2/min^2

V = volume of one compartment in aerosol chamber, ft^3

x = rectangular coordinate parallel to vertical direction in aerosol chamber

y = rectangular coordinate transverse to opening between compartments of aerosol chamber

$\overline{y^2}$ = statistical dispersion length defined by equation (3.25), $in.^2$

α_t = turbulent thermal diffusivity, $in^2/min.$

β = coefficient defined in equation (3.40).

θ = temperature, °F.

θ_a = absolute temperature, °R.

ν = kinematic viscosity, in^2/min

ν_t = turbulent viscosity, in^2/min

ξ = time lag in instantaneous velocity correlations, sec

Bar above symbol indicates mean component

Prime above symbol indicates instantaneous component

Subscripts:

H refers to compartment with highest magnitude

L refers to compartment with low magnitude

1. INTRODUCTION

A small percentage of the 1,500,000 particles in an average cubic foot of air are viable microorganisms. However, the existence of these viable bacteria in the air of dairy and food processing plants is of greater importance than the small percentage indicates. Reports on the populations of air-borne microorganisms are varied both in approach and results. Olson and Hammer (1934) and Cerna (1961) reported counts as high as 12 and 55, respectively, settling on a standard size petri dish per minute in various areas of dairy plants. Labots (1961) and Heldman _et al_. (1964) reported mean counts of 5 to 85 per ft^3 when using vacuum slit samplers. The fact that populations of air-borne microorganisms exist in food processing areas can be attributed to the many sources present in these areas. Isolation of floor drains as a source of air-borne microorganisms during flooding is just one example (Heldman _et al_., 1965).

The existence of an air-borne microorganism population of any magnitude provides a chance for air-borne contamination of exposed products. In many cases, this contamination may occur after processing and will result in significant reductions in product shelf-life. The importance of this type of contamination is increasing significantly due to the prospects of packaging sterile products such as milk and other milk products. Contamination of the sterile product with a single microorganism will result in an unacceptable storage life for these products.

The development of ultra-high efficiency or ABSOLUTE filters for air may solve at least part of the air-borne contamination problem. These filters, which are designed to remove 99.97% of all 0.3 micron particles, will provide air which is practically free of air-borne microorganisms. However, the more difficult and unsolved problem is that of secondary contamination or contamination of the filtered air from the many sources of air-borne microorganisms in the processing plant. A partial solution to the latter problem is localized control by use of "laminar air flow" (Whitfield, 1963) or jets of filtered air to protect selected spaces. These mthods are limited, however, to small spaces and much is unknown about the effectiveness of laminar air flow in the mixing regions.

Before complete control of air-borne contamination can be attained, basic information on the transport of air-borne microorganisms from the source to the product must be obtained. Within a room, the movement and flow patterns of the air is of major concern. However, when considering transport of air-borne microorganisms from one room to an adjoining room, factors such as the mixing of two air streams at openings between rooms is of importance. Unless there is considerable momentum transport or air movement through the openings, the mixing of the air streams must provide the major portion of the transport. In addition, the mixing of a high concentration air stream with a low concentration air stream may be influenced by other variables such as flow conditions of the air streams, geometry at the initial point of mixing and differences in temperature and relative humidity between the air streams.

The purpose of this investigation is to determine the transport characteristics of air-borne microorganisms in a mixing region which would simulate that encountered between two rooms with different air-borne concentrations. The results obtained should not be limited to food and dairy processing plants because of the wide-spread interest in the same subject in hospitals and "dust free" rooms. Mixing regions are also encountered in many contamination control devices, and results obtained in this investigation may lead to improved control methods.

2. LITERATURE REVIEW

2.1 Characteristics of Air-Borne Bacteria

The development of procedures and techniques for the study of air-borne bacteria has occurred, to the greatest extent, in the last 15 to 20 years. The stimulation of these developments has been related mostly to: (a) increased frequency of air-borne infection by antibiotic resistant strains of bacteria in hospitals and (b) the possibilities of biological warfare.

2.1a Existence

Air-borne bacteria exist as aerosols, which are defined as liquid or solid particles in air. According to Wolf, *et al*. (1959), the biological particles may exist in any of the following forms: (a) single unattached cells, (b) clumps composed of a number of microorganisms, (c) cells adhering to a dust particle, or (d) a free floating microorganism surrounded by a film of dried organic or inorganic material. In addition, the microorganism involved may be a vegetative cell or a spore. The relative importance of vegetative cells as compared to spores depends on the air space involved. Wolf, *et al*. (1959) indicates that vegetative cells are of greater importance when concerned with communicable diseases. However, air-borne contamination of a processed food by spores is of equal importance, since the conditions are usually ideal for germination.

2.1b Sedimentation and Deposit

An air-borne microorganism is subjected to the influence of gravity and the motion of the surrounding fluid. Most evidence (Decker, *et al.*, 1962) indicates that air-borne microorganisms, other than viruses, are 0.3 micron in diameter or larger. According to Wells (1955), particles of this size will settle from the air in a manner described by Stokes's law. Tanner (1963) and DallaValle (1948) express this law as:

$$v_g = \frac{(\rho_p - \rho_g)\ g\ d^2 c}{18\mu} \tag{2.1}$$

where:

v_g = terminal velocity of aerosol particles

ρ_p = density of aerosol particles

ρ_g = density of air,

g = gravitational constant

d = diameter of aerosol particles

μ = viscosity of air

The Cunningham "slip" correction factor (c) is proportional to the mean free path of the gas molecules and becomes increasingly important for particles less than 20 microns in diameter. Tanner (1963) discusses the difference between quiescent and turbulent aerosols and indicates that Stokes equation (2.1) will apply in both conditions. In general, a quiescent aerosol will "fall-out" at the constant rate of particle fall described by Stoke's equation (2.1). A turbulent aerosol possesses a constant rate of fallout of particles, which is proportional to the rate of particle fall (v_g) and the aerosol concentration. Tanner (1963) assumes that deposit on walls and ceiling of a chamber is negligible, and developed the following equation for evanescence of a quiescent aerosol:

$$\left(\frac{C}{C_0}\right)_Q = 1 - \frac{v_g t}{h} \tag{2.2}$$

Both Wells (1955) and Tanner (1963) described the sedimentation of a turbulent aerosol as:

$$\left(\frac{C}{C_0}\right)_T = 1 - \exp\left(- \frac{v_g t}{h}\right) \tag{2.3}$$

where:

C = concentration of aerosol at any time, t

C_0 = concentration of aerosol at t = 0.

v_g = terminal velocity of aerosol particles.

h = height of aerosol chamber

The fact that aerosol particles will deposit when subjected to certain conditions is demonstrated by Porter, et al. (1963) while studying the decay of an aerosol moving through a duct. Experimental results indicated that this decay or deposit was a function of particle size, velocity and duct size.

2.1c Viability

Although some air-borne spores may have nearly unlimited viability, the viability of a vegetative cell will be limited depending on the conditions to which it is exposed. The death of vegetative cells is expressed by Wells (1955) in the following manner:

$$\mathrm{Ln}\left(\frac{C}{C_0}\right) = -Kt \qquad (2.4)$$

where:

K = death rate constant

t = time

Here the death rate constant (K) is dependent on many factors such as bacterial species, air temperature and relative humidity.

The factors affecting the viability of air-borne bacteria have been studied in detail by Webb (1959). When aerosols consisted of bacterial cells from distilled water, the death of the cells appeared to occur in two stages; rapid loss in viability during the first second followed by a slower death rate which obeyed first order kinetics at low relative humidities. The results suggested that death of the cells resulted from movement of water molecules in and out of the cell, in an equilibrium system, resulting in a collapse of the natural structure of cellular protein. Wells (1955) indicated that, in general, the initial death rate is higher in dry air, but longevity of survivors appears to be greater in dry air than in moist air.

Experimental determination of death rate constants was conducted by Kethley, et al. (1957) for bacterial aerosols of *Serratia marcescens*. The determinations were made in an aerosol chamber and by use of equation (2.4). The results obtained are presented in Table 2.1

TABLE 2.1.--Influence of relative humidity on death rate constants of *Serratia marcescens*.

Relative Humidity	Washed Cells Dispersed from Water		Cells Dispersed from 0.3% Beef Extract Broth	
	Ave. K	S. E.	Ave. K	S. E.
%	(1/min)		(1/min)	
16	0.021	0.0008		
20	0.032	0.0020	0.020	0.0050
25	0.040	0.0010	0.020	
40	0.060	0.0030	0.025	
52			0.025	0.0003
60	0.044	0.0020	0.032	0.0020
80			0.008	0.0003
90	0.036	0.0020		
95	0.021	0.0010		

The results (Table 2.1) illustrate the influence of relative humidity on death rate constants for *Serratia marcescens* dispersed from different types of aqueous media. The types of media were selected to represent the conditions surrounding an air-borne bacteria. The results indicate that the maximum death rate for both plain bacterial cells and cells surrounded by proteinaceous material occurs between 40 and 60% relative humidity. However, it is evident that cells dispersed from beef extract broth had lower death rates than cells dispersed from distilled water, indicating a protective influence of the material surrounding the cell.

2.1d Sampling

The methods available for sampling air-borne micro-organisms are very similar to those used for other air-borne particles. According to Wolf, et al. (1959), the methods can be grouped as follows: (a) impingement in liquids, (b) impaction on solid surfaces, (c) filtration, (d) sedimentation, (e) centrifugation, (f) electrostatic precipitation and (g) thermal precipitation. All methods used for air-borne particles must be modified to allow for recovery of living biological particles.

The methods for sampling and evaluation of air-borne biological particles are discussed by Wolf, et al. (1959). In general, methods employing the impingement on liquid principle have very high efficiencies for collecting and enumerating the bacterial cell suspended in air. However, high impingement velocities may result in losses of viability of vegetative cells. Methods which sample air by use of filtration will provide collection efficiencies as high as the efficiency of the filter media. The methods tend to be somewhat more suitable for spores and other resistant microbial forms since vegetative cells may not resist desiccation associated with filter collection.

Sedimentation is probably the most inexpensive and simple method for determining the microbiological quality of air. However, the method has the serious disadvantage of being selective for larger air-borne particles and not the entire particle-size distribution. In addition, the influence of air movement prevents an accurate correction of this factor. For the results obtained by the sedimentation technique to be of quantitative value, the aerosol must be allowed to settle quiescently onto a collecting surface in a closed container. Due to the long periods of time required for settling, vegetative cells lose viability before reaching the surface.

Centrifugation was one of the first successful methods developed for quantitatively evaluating air-borne bacterial populations (Wells, 1933). Although the efficiency may be very high, it is dependent on operating conditions and particle size. Two of the more complex sampling methods described by Wolf, et al. (1959) are the electrostatic and thermal precipitation samplers. The electrostatic unit provides high collection efficiency at relatively high sampling rates, but the instrument is complex and requires careful attention to maintain accuracy. Thermal precipitation samplers are complex also and sampling rates are very low.

Wolf, _et al_. (1959) describes impaction samplers as best adapted to determining the concentration of particles which contain bacterial cells. One of the impaction samplers commonly used is the slit sampler which allows collection of the viable particles on an agar surface. Bourdillon, _et al_. (1941) found the slit samplers to be highly efficient for the smallest bacteria-carrying particles, under the proper conditions (air flow, slit width, and distance of slit from surface).

2.2 Production and Study of Uniform Bacterial Aerosols

To study the characteristics of a bacterial aerosol, two factors are desirable: (a) production of bacterial particles which are similar to those normally present in air-borne populations and (b) control of aerosol concentration and distribution by using an aerosol chamber.

2.2a Production of the Aerosol

According to Greene (1965), it is impossible to experimentally produce an aerosol which simulates normal conditions because of the manner in which air-borne micro-organisms normally exist. Decker, _et al_. (1962) reviews methods used to produce bacterial aerosols such as small glass or plastic atomizers. With such devices, it is possible to produce aerosols containing a high percentage of particles approximately 1 micron in diameter. Wells (1955) points out that production of an aerosol involves two stages: (a) atomization involving the formation of liquid droplets containing bacterial cells and/or associate particles and (b) evaporation of the liquid as described by Raoult's Law. Although Greene (1965) indicated that more experimental work is being conducted using lyophilized culture powders, Kethley, et al. (1956) and Porter, et al. (1963) have had reasonable success by atomizing liquid cultures into a prechamber. The prechamber provided conditions for evaporation of liquid portion of the particles and sedimentation of large particles. Using this technique, with 0.3% beef extract culture media, Kethley, et al. (1956) were able to produce aerosols with average particle sizes ranging from 1.8 microns at 25% relative humidity to 2.3 microns at 80% relative humidity. The aerosol contained particles which had no more than two bacterial cells with 90% of the particles containing only one cell. Porter, et al. (1963) reported experiments with aerosols which contained between 1 and 8 microns when using similar techniques. In general, Kethley, et al. (1957) concluded that aerosol particle sizes could be predicted on the basis of the atomized droplet volume, the concentration of solids or low vapor pressure liquids in the dispersed media and the response of the components to relative humidity.

2.2b The Aerosol Chamber

The more prevalent and well-known uses of aerosol chambers include the study of air-borne infection (Druett and May, 1952; Henderson, 1952; Laurell, et al., (1949; Leif and Krueger, 1950; Robertson, et al., 1946; Rosebury, 1947; Urban, 1954; Weiss and Stegeler, 1952) and the effectiveness of various germicidal agents (DeOme et al., 1944); Kaye, 1949; Mackay, 1952; Rentschler, 1942; Twort, et al., 1940) However, chambers designed for the mentioned purposes are not well adapted for studying the nature and composition of bacterial aerosols during long time trials. A chamber which is well suited to the latter purpose was designed by Kethley, et al. (1956). Experimental results indicated that the chamber designed would allow an increase in aerosol concentration according to the standard ventilation equation (Silver, 1946):

$$C = C_0 \left[1 - \exp\left(- \frac{ft}{V}\right)\right] \tag{2.5}$$

and would produce disappearance of the aerosol by a similar equation:

$$C = C_0 \left[\exp\left(- \frac{ft}{V}\right)\right] \tag{2.6}$$

Kethley, et al. (1957) proved that the aerosol concentration in the chamber was uniformly distributed by determining concentrations at points throughout the chamber. In addition, the ability of the chamber to maintain a consistent concentration for long periods of time was tested by sampling at intervals up to 130 minutes.

2.3 Transport Processes

Crank (1956) states that diffusion is the process by which matter is transported from one part of a system to another as a result of random molecular motions. Hinze (1959) shows that transport of a transferable quantity by random fluid motion is diffusive in nature. Since turbulent fluid motion is a random fluid motion, the transport of matter in a turbulent fluid must involve both molecular and turbulent diffusion (Frenkiel, 1953). Crank (1956) states Fick's law of diffusion as:

$$F = - D \frac{\partial C}{\partial x} \tag{2.7}$$

where F represents mass flux and, in the case of diffusion due to turbulent motion, D represents the sum of the molecular diffusion coefficient and the eddy diffusivity.

2.3a Turbulence

Hinze (1959) presents the following definition: "Turbulent fluid motion is an irregular condition of flow in which the various quantities show a random variation with time and space coordinates, so that statistically distinct average values can be discerned." As many authors (Hinze, 1959; Schlichting, 1960) indicate, there are distinct differences between turbulence generated by friction forces at fixed walls (wall turbulence) and that generated by the flow of layers of fluid with different velocities past or over one another (free turbulence).

Most frequent theoretical approaches to the study of turbulence involves the assumption of isotropic turbulence (Hinze, 1959; Townsend, 1956; Frenkiel, 1953). Although this type of flow is ideal and does not exist except under local conditions, its value is that it may provide a fundamental basis for the study of the types of turbulence which actually exist. According to Frenkiel (1953) the term isotropic implies that the statistical characteristics of the flow will be invarient under rotation or reflection of the axes. This basic approach to the study of turbulence was begun by Taylor (1921) and has resulted in a definite trend toward the study of the statistical properties of turbulence rather than the use of phenomenological theories, which describe the influence of mean flow only.

The term homogenious turbulence is frequently used to describe the turbulent field in which the statistical characteristics are not changed by translation of the axes (Frenkiel, 1953). This type of turbulence exists in real situations, but will form a part of a nonisotropic or anisotropic turbulence. As revealed by Hinze (1959), the contributions to the theory of nonisotropic are small due to the extreme complexity of the problem.

According to Townsend (1956), nonhomogenious turbulent flow exists primarily in the following: (a) in the boundary regions between a field of homogenious turbulence and an adjacent undisturbed field, (b) when turbulent intensities and other quantities are symmetrical about a plane and (c) when turbulent intensities and other quantities are axisymmetric. As would be expected, theoretical development of inhomogenious turbulence is at an early stage.

2.3b Turbulent Diffusion

The basic transport mechanisms of momentum, heat and mass in turbulent flow are very similar. According to Pasquill (1962), the theoretical treatment of the turbulent diffusion of these quantities has proceeded according to two approaches: (a) transfer theory in which the transport rate is proportional to a concentration gradient with a proportionality factor or constant and (b) statistical description in which an analytical technique for representing the history of the fluid elements in terms of the statistical properties of the turbulent motion is used. Schlichting (1960) points out that the first approach (transfer theory) involves calculations based on empirical hypothesis which endeavors to establish a relationship between the Reynold's stresses produced by mixing motions, and the mean values of the velocity components together with suitable hypothesis concerning heat and mass transfer.

According to Hinze (1959), the more complete and correct solution to turbulent flow problems can be obtained by expressing the turbulent-transport rate of the transferable quantity completely in terms of statistical functions of the turbulent velocity field and of boundary or initial conditions.

The basic concepts of transfer theory in turbulent flow were introduced by Boussinesq (1877) who described Reynold's stress in turbulent flow by:

$$T_t = A_T \frac{\partial \bar{u}}{\partial y} \tag{2.8}$$

where A_T is called a mixing coefficient which is dependent on the mean velocity. A similar relationship for transfer of mass in turbulent flow:

$$F = - \bar{\rho} \; K \frac{\partial \bar{s}}{\partial y} \tag{2.9}$$

was proposed by Pasquill (1962), with K equal to the proportionality constant and $\frac{\partial \bar{s}}{\partial y}$ equal to the concentration gradient. In order to use the preceding equations, it is necessary to have knowledge of the manner with which the coefficients vary with the mean velocity or other measureable quantity. One of the most useful concepts in the description of turbulent-transport processes is the "mixing length" theory introduced by Prandtl (1925). Prandtl's mixing length hypothesis is:

$$T = \rho \; \ell^2 \left| \frac{d\bar{u}}{dy} \right| \frac{d\bar{u}}{dy} \tag{2.10}$$

where T is shear stress and ℓ is a mixing length described as the distance in the transverse direction which must be covered by an agglomeration of fluid particles traveling with its original mean velocity in order to make the difference between its velocity and the velocity in the new lamina equal to the mean transverse fluctuation in turbulent flow. As indicated by Hinze (1959), the "mixing length" does not describe turbulent flow entirely correctly but does provide a useful tool for calculation purposes.

A second and similar transfer theory was introduced by Taylor (1915). This second theory differs from Prandtl's momentum transport theory in that it describes the diffusion of vorticity rather than momentum. Schlichting (1960) indicates that this theory has particular application in free turbulent flow. Taylor (1932) has shown that the momentum transport and vorticity transport theories agree when turbulent motion is two-dimensional and confined to the plane perpendicular to the mean motion. However, when turbulent motion and mean motion are confined to two-dimensions, the results of the two theories differ significantly. The differences between the two theories are evident again when comparing velocity and temperature or concentration distributions in wakes or free turbulent mixing regions. The momentum transport theory would predict the distributions to be identical. Taylor's vorticity transport theory predicts different distributions which have been confirmed experimentally by Fage and Falkner (1932).

If the turbulent flow is assumed homogenious and isotropic, solutions to the parabolic equation of diffusion become very useful. This equation, as presented by Pasquill (1962),

$$\frac{\partial C}{\partial t} = \frac{\partial}{\partial x}\left(K_x \frac{\partial C}{\partial x}\right) + \frac{\partial}{\partial y}\left(K_y \frac{\partial C}{\partial y}\right) + \frac{\partial}{\partial z}\left(K_z \frac{\partial C}{\partial z}\right) \qquad (2.11)$$

with K_x, K_y, K_z equal to eddy diffusivities in various coordinates, can be adapted and solved for a given set of conditions. Several such solutions for point or line sources of concentration are presented by Frenkiel (1953) and Hinze (1959).

Experimental investigations involving turbulence and turbulent diffusion have been concerned mainly with the description of eddy diffusivities in terms of mean flow. Towle and Sherwood (1939) determined eddy diffusivities for turbulent flow in ducts and found that values increased proportionately to Reynolds' number. In addition, the results indicated that the scale of turbulence in free duct flow is significantly larger than that produced by a grid. Results presented by Sherwood and Woertz (1939) show that the eddy diffusivity is essentially constant over the central portion of a turbulent gas stream in a duct. The product of eddy diffusivity and gas density was found to be about 1.6 times larger than the eddy viscosity. A semi-theoretical relationship was established relating the eddy diffusivity to mean velocity, duct radius and the friction factor. The importance of having knowledge of the scale of turbulence is revealed in investigations by Kalinske and Pien (1944). Results revealed that the eddy diffusivity is directly related to the scale of turbulence, which must be measured to provide an accurate prediction of the turbulent diffusion.

A statistical description of the turbulent field is required in order to accurately solve a turbulent transport problem. The basic concepts involved in statistical theory of turbulence were introduced by Taylor (1921) and developed by Taylor (1935). In general, the statistical concept involves the correlation between the velocity of a particle at one time and that of the same particle at a later time, or the correlation between simultaneous velocities at two fixed points.

Statistical aspects of turbulent flow are reviewed by Frenkiel (1953), Hinze (1959), and Pasquill (1962). Basically, turbulent flow cannot be described by a mean velocity, only, since the velocity fluctuations around the mean velocity are an indication of the intensity of turbulence. Usually, the instantaneous velocity is represented by:

$$u = \bar{u} + u' \qquad (2.12)$$

where u' represents the turbulent velocity or instantaneous difference from the time mean velocity $\bar{u}$ and such that $\overline{u'} = 0$. However, since the turbulent velocity changes continuously with time, Dryden and Kuethe (1930) suggested the use of the root mean square value $\sqrt{\overline{u'^2}}$. The intensity of turbulence, degree of turbulence or turbulence level is then defined as $\frac{(\overline{u'^2})^{\frac{1}{2}}}{\bar{u}}$ for the longitudinal direction and $\frac{(\overline{v'^2})^{\frac{1}{2}}}{\bar{u}}$ would be the transverse intensity of turbulence.

Turbulent transport processes may be statistically described in two ways according to Hinze (1959). The Eulerian description involves the variation of some property with respect to a fixed coordinate system. The variation of the property connected with a given fluid particle or fluid lump while moving through the flow field is the Lagrangian description. Frenkiel (1953) defines the Eulerian longintudinal correlation coefficient for velocity as:

$$R_x(x) = \frac{\overline{u_P' \quad u_Q'}}{\sqrt{\overline{u_P'^2}} \quad \sqrt{\overline{u_Q'^2}}} \tag{2.13}$$

The value of this correlation coefficient will range from one when the points (P and Q) coincide to zero when the points are far apart. A similar correlation coefficient can be calculated in the transverse direction. The Eulerian time correlation coefficient would be defined as:

$$R_t(h) = \frac{\overline{u'_p(t) \quad u'_p(t+h)}}{\sqrt{\overline{u'_p(t)^2}} \quad \sqrt{\overline{u'_p(t+h)^2}}} \tag{2.14}$$

where h represents the time lag between instantaneous velocities at the same point.

Frenkiel (1953) defines the Lagrangian correlation coefficient in the longitudinal direction as:

$$\overset{u}{R}_{tL}(h) = \frac{\overline{u'_A(t) \quad u'_A(t+h)}}{\sqrt{\overline{u'_A(t)^2}} \quad \sqrt{\overline{u'_A(t+h)^2}}} \tag{2.15}$$

This correlation coefficient corresponds to a Lagrangian time-scale of turbulence:

$$\overset{u}{L}_{tL} = \int_0^{\infty} \overset{u}{R}_{tL}(\alpha) \, d\alpha \tag{2.16}$$

A similar Lagrangian length-scale of turbulence can be calculated based on the distance traveled during time (h). According to Taylor (1935) this length is analogous to Prandtl's mixing length. The corresponding Eulerian length-scale is an indication of the average eddy size.

Additional description of turbulent flow is obtained by determination of the spectrum which measures the relative contribution of various frequencies of velocity fluctuations to turbulent energy. Frenkiel (1953) defines the longitudinal spectrum of turbulence as:

$$F_x(k') = \frac{2}{\pi} \overline{u'^2} \int_0^{\infty} R_x(s) \cos(k's) \, ds \tag{2.17}$$

where the function $[F_x(k')]$ represents the contribution to $\overline{u'^2}$ at the wave number k'.

The dispersion of a fluid element or particle in turbulent flow is usually described in terms of the variance of the coordinate system components ($\overline{x^2}$, $\overline{y^2}$, or $\overline{z^2}$). Assuming homogenious isotropic turbulence, Frenkiel (1953) derived the fundamental equation of turbulent diffusion:

$$\overline{y^2} = 2\ \overline{v^2} \int_0^t (t-\alpha)\ R_h\ (\alpha)\ d\ \alpha \qquad (2.18)$$

where α is equal to time lag used for calculating $R_h\ (\alpha)$. When dispersion time is large compared to the Lagrangian time-scale of turbulence (equation 2.16) the correlation coefficient becomes very small and equation 2.18 becomes:

$$\overline{y^2} \approx 2\ \overline{v^2}\ L_h t \qquad (2.19)$$

If dispersion time is small compared to the Lagrangian time-scale (L_h), Frenkiel (1953) has derived the expression:

$$\overline{y^2} \approx \left[1 - \frac{1}{6}\frac{t^2}{\lambda_h^2}\right] \overline{v^2}\ t^2 \qquad (2.20)$$

or when dispersion time is small compared to the microscale of turbulence λ_h:

$$\overline{y^2} \approx \overline{v^2}\ t^2 \qquad (2.21)$$

For the case when dispersion time neither large nor small compared the Lagrangian time-scale, Frenkiel (1953) introduces a dispersion factor:

$$i = \frac{1}{L_h} \sqrt{\frac{\overline{y^2}}{\overline{v^2}}} \tag{2.22}$$

Further description of the turbulent flow involves representing the correlation curve by known functions.

If $\nu_t = \overline{v^2}\, L_h$ and dispersion time is large, equation 2.19 becomes:

$$\overline{y^2} \approx 2\nu_t t \tag{2.23}$$

and the eddy diffusion (D_t) becomes:

$$D_t = \nu_t + \nu \tag{2.24}$$

when the molecular diffusivity coefficient is assumed equal to the kinematic viscosity.

Frenkiel (1953) defines a factor of turbulent diffusion:

$$n = \tfrac{1}{2} \frac{d(\overline{y^2})}{dt} = \overline{v'^2} \int_0^t R_h(\alpha)\, d\alpha \tag{2.25}$$

By replacing the constant eddy diffusivity in the diffusion equation with the above factor (n), the equation becomes valid for a large number of dispersion times (Pasquill, 1962).

Since Fick's diffusion equation is not valid even in homogenious isotropic turbulence, experimental eddy diffusivities obtained in this manner can only represent apparent coefficients for conditions studied. Frenkiel (1953) explains that the ratio of the apparent coefficient to the real eddy diffusivity is related to the statistical properties of the turbulence:

$$\frac{D_a}{D_t} \simeq \frac{\nu_a}{\nu_t} = \frac{i^2}{2T} \tag{2.26}$$

The ratio is then a function of relative dispersion time ($T = t/L_h$) and shape of the Lagrangian correlation curve.

2.3c Transport in Mixing Regions

Typical examples of free turbulent flow and the corresponding mixing which occurs are reviewed by Schlichting (1960). A free jet boundary occurs between two streams which are moving at different speeds in the same direction. A free jet occurs when a fluid is discharged from a nozzle or orifice. The turbulent region behind a solid body moving through a fluid or a solid body in a stream of air is called a wake. These types of free turbulent flow can be described by boundary layer equations which have been solved for various sets of conditions by Schlichting (1960) and Pai (1954).

A basic requirement for the description and solution of turbulent mixing problems is knowledge of the velocity distribution. Goldstein (1930) provided a detailed solution to the boundary layer equations for two-dimensional steady motion. Howarth (1934) and Tomotika (1938) used the vorticity transfer theory to describe the velocity distribution in plane and axially symmetrical jets. Results revealed an identical distribution when compared to momentum transfer theory, but the authors concluded that experimental temperature distributions would be required to test both theories. Kuethe (1935) assumed that Prandtl's mixing length is proportional to the breadth of the turbulent mixing region and obtained solutions for velocity fields for mixing of two parallel streams of different velocities and for an axially symmetrical jet. Albertson, et al. (1948) used three assumptions to solve for the flow pattern in a submerged jet. The assumptions were: (a) the pressure is hydrostatically distributed throughout the flow; (b) the diffusion process is dynamically similar under all conditions; and (c) the longitudinal component of velocity within the diffusion region varies according to the normal probability function at each cross section. Experimental results indicated validity of the assumptions. Pai (1949) solved the equation of motion for the mixing region of a two-dimensional jet and obtained a solution containing the Gaussian error function. Lock (1951) obtained solutions for the velocity distribution in the laminar boundary layer between two parallel streams which differ in density and viscosity. Results indicated that the solutions depend on the ratio of the velocities of the two streams and the product of the viscosity and density ratios. Torda, et al. (1953) used the von Karman integral concept to analyze the turbulent incompressible symmetric mixing of two parallel streams. The velocity distribution in the mixing region and the thickness of the region was evaluated while accounting for the influence of the upstream boundary layers.

Pai (1955) solved the equations for two-dimensional and axially symmetrical turbulent jet mixing of two gases at constant temperature assuming constant exchange coefficients in the mixing region.

A second essential requirement for study and description of turbulent transport of quantities other than momentum is the concentration distribution. The concentration distribution for a circular jet with annular coaxial stream was measured by Forstall and Shapiro (1950). The results indicated that concentration diffuses more rapidly than momentum. Pai (1954) compared theoretical equations with experimental results and indicated that for mixing regions far downstream, the concentration profiles can be represented by error functions. Pai (1956) presented solutions to laminar jet mixing problems for velocity, temperature, and concentration distributions. In general, all solutions contain some form of the error function. Batchelor (1957) discusses the statistical characteristics of diffusion in jets, wakes, and mixing layers. The author's hypothesis is that the velocity of a fluid particle in free turbulent shear flow exhibits a corresponding Lagrangian similarity and can be transformed to a stationary random function. Csanady (1963) solved a differential equation derived from the energy balance of the mixing layer and obtained solutions for turbulent intensity profiles which agreed with experiments.

Several investigations have dealt specifically with velocity and concentration distributions in mixing regions created by wakes. Goldstein (1933) presented the calculations of the velocity distribution in the wake behind an infinitely thin plate parallel to a fluid stream. Hollingdale (1940) and Townsend (1949) have presented theoretical and experimental results which describe velocity distributions and transport in the wake mixing regions. The validity of the mixing length theory for turbulent shear flow has been questioned. Experimental results, reviewed by Batchelor (1950) presents general mechanisms for transfer of momentum, turbulent energy and heat. However, analytical theory corresponding to the experimental results has not been formulated. Cheng and Kovitz (1958) present solutions to the initial value problem involving mixing and chemical reaction in a laminar wake of a flat plate. Coles (1956) proposes the use of universal flows to describe the mean velocity profile of two-dimensional incompressible turbulent boundary layer flows. The wake model for free-streamline flow is used by Wu (1962) to treat the two-dimension flow past an obstacle with wake or cavity formation.

3. THEORETICAL CONSIDERATIONS

The transport of air-borne bacteria through an opening between two rooms with different concentrations probably involves many mechanisms acting individually or simultaneously. For purposes of this investigation, a theoretical mixing region model will be proposed. The model consists of two different uniform concentrations of air-borne bacteria separated by a partition. The two-dimensional mixing region is located at an opening in the partition through which transport of the aerosol occurs. The opening is considered infinitely long in the direction perpendicular to air flow past both sides. The mechanism of transport considered is the turbulent dispersion of the high concentration aerosol into the low concentration air and the subsequent entrainment on the low concentration side of the model. The analysis of the model involves consideration of several factors:

a. Equal air flow on both sides of the model--this analysis will involve determination of dispersion in highly turbulent air moving at low flow rates typical of ventilation systems. Depending on the intensity of turbulence in the free stream, the influence of turbulence created by a wake of the partition may need to be considered.

b. Unequal air flow across the mixing region--a complete analysis of this case involves several considerations. Due to unequal flow, the possibilities of momentum transport through the mixing region and variation of turbulence across the mixing region must be taken into account.

c. Variation in opening size--the height of opening in the same direction as the air flow will have a direct influence on the extent of dispersion. In addition, any influence of opening size on turbulence characteristics should be established.

d. Width of partition--the width of the partition at the initial point of mixing will require at least two considerations. One is the possibility of increased turbulence due to the wake. The other is a reduction in dispersion length due to the increased width at the initial point of mixing.

e. Temperature gradient--the primary considerations involving temperature gradient are the influence on viability of the aerosol and the possibility of increased convective currents.

In order to allow an analysis which lends itself to mathematical ease and clarity, several assumptions are required:

a. The particle size of the bacterial aerosol is uniform, i.e., the influence of transport mechanisms and gravitational forces is the same for all particles.

b. The die-away characteristics of all particles in the aerosol are uniform.

c. The influence of a mean pressure gradient existing at the opening is negligible.

d. Transport due to molecular effects is very small compared to turbulent transport, i.e., Brownian motion is negligible.

e. Turbulence in the mixing region is isotropic, i.e., $\overline{u'^2} = \overline{v'^2} = \overline{w'^2}$.

f. The differences in temperature encountered are sufficiently small to allow the use of constant fluid properties.

The first two assumptions are based on work conducted by Kethley, et al. (1956) with experimentally generated *Serratia marcescens*. These assumptions would rarely apply under actual conditions, but they are necessary simplifying assumptions which can be met experimentally. The third, fourth and fifth assumptions depend primarily on the intensity of turbulence which exists in the mixing region. The model specifies sufficient turbulence to maintain uniform aerosol concentrations on both sides of the partition; therefore, the indicated assumptions would appear to be good. Since a 20°F. temperature gradient will produce less than five per cent change in the properties of air, the last assumption can be used without major concern.

3.1 Basic Diffusion Equations

The two-dimensional mixing region described in the model is not unlike the laminar or turbulent jet boundary described frequently in fluid mechanics literature. In most cases, the mixing region formed by the two parallel streams is treated as a boundary layer and the same simplifying assumptions to the basic equations are adopted (Schlichting, 1960). Using this approach the transport in the mixing region model can be described by the following steady-flow equations:

a. Equation of motion:

$$\bar{u}\,\frac{\partial \bar{u}}{\partial x} + \bar{v}\,\frac{\partial \bar{u}}{\partial y} = \nu\,\frac{\partial^2 \bar{u}}{\partial y^2} \tag{3.1}$$

b. Equation of turbulent energy:

$$\bar{u}\,\frac{\partial \overline{u'^2}}{\partial x} + \bar{v}\,\frac{\partial \overline{u'^2}}{\partial y^2} = \nu_t\,\frac{\partial \overline{u'^2}}{\partial y^2} \tag{3.2}$$

c. Equation of diffusion:

$$\bar{u}\,\frac{\partial C}{\partial x} + \bar{v}\,\frac{\partial C}{\partial y} = D_a\,\frac{\partial^2 C}{\partial y^2} \tag{3.3}$$

d. Equation of energy:

$$\bar{u}\,\frac{\partial \theta}{\partial x} + \bar{v}\,\frac{\partial \theta}{\partial y} = \alpha_t\,\frac{\partial^2 \theta}{\partial y^2} \tag{3.4}$$

e. Equation of continuity:

$$\frac{\partial \bar{u}}{\partial x} + \frac{\partial \bar{v}}{\partial y} = 0 \tag{3.5}$$

These equations should completely describe the turbulent transport of aerosol particles in the model proposed. The solution to the equation of motion will describe changes in mean velocity across the mixing region when unequal air flows are analyzed. The very low magnitudes of the mean air velocity and small differences in mean air velocity between the two sides should allow treatment of the mixing region as a laminar jet boundary and the use of known fluid properties for air.

The proposed model requires sufficient turbulence to maintain homogeneous concentrations on both sides of the mixing region. This turbulence must be superimposed on the low mean velocities which exist, and therefore moves slowly past the mixing region. The proposed equation of turbulent energy describes the distribution of the statistical turbulent energy factor ($\overline{u'^2}$). This distribution becomes particularly important in cases where a gradient of the turbulent energy exists across the mixing region model.

The equations of diffusion and energy are proposed in order to describe distributions of concentration and temperature in the model mixing region. Because the proposed model considers only transport due to turbulent effects, the constants, D_a and α_t will be referred to as apparent eddy diffusivity and turbulent thermal diffusivity, respectively. The continuity equation specifies that conservation of mass exists in the mixing region.

The purpose of the proposed mixing region model is to provide some theoretical basis for the transport of a bacterial aerosol through an opening in a partition separating two different concentrations. To provide mathematical ease in the description of this transport, it would be desirable to obtain closed solutions to the equations which represent the distribution of the various parameters in the mixing region. One approach to attaining this objective is to make additional assumptions with respect to flow conditions in the mixing region. The assumption that $\overline{v} = 0$ should be valid based on specifications of the model. As indicated, the overall movement of air past the opening is in the downward (+x) direction. All other components of air movement are turbulent fluctuations. Therefore, the only non-negative mean velocity is $\overline{u}$ (x-component). The assumption that $\overline{v} = 0$ simplifies the previous equations considerably and thus they may be stated in the following manner:

a. Equation of motion:

$$\overline{u} \frac{\partial \overline{u}}{\partial x} = \nu \frac{\partial^2 \overline{u}}{\partial y^2} \tag{3.6}$$

b. Equation of turbulent energy:

$$\overline{u} \frac{\partial \overline{u'^2}}{\partial x} = \nu_t \frac{\partial^2 \overline{u'^2}}{\partial y^2} \tag{3.7}$$

c. Equation of diffusion:

$$\bar{u} \frac{\partial C}{\partial x} = D_a \frac{\partial^2 C}{\partial y^2} \tag{3.8}$$

d. Equation of energy:

$$\bar{u} \frac{\partial \theta}{\partial x} = \alpha_t \frac{\partial^2 \theta}{\partial y^2} \tag{3.9}$$

The equations of interest are now reduced to more simple forms similar to the heat conduction equation. Such equations have been used frequently by Pai (1949, 1955, 1956) to obtain solutions which describe velocity distributions in laminar and turbulent jet mixing regions.

More firm support for the use of the preceding equations in regions of free turbulence was provided by Reichardt (1941, 1944). Reichardt's inductive theory of turbulence is derived almost completely from experimental evidence, which indicates that velocity profiles in free turbulent flows can be approximated very successfully by the Gaussian error function. Reichardt's fundamental equation for describing the velocity distribution in free turbulent flow is:

$$\frac{\partial \overline{u^2}}{\partial x} = \Lambda(x) \frac{\partial^2 \overline{u^2}}{\partial y^2} \tag{3.10}$$

where Λ is a momentum transfer length. The similarity of Reichardt's equation and equations proposed for use in this investigation is apparent.

Solutions to equations 3.6, 3.7, 3.8, and 3.9 can be obtained by use of boundary conditions which describe the model mixing region. These boundary conditions can be stated as follows:

At $x = 0$, $y > 0$:

$$\bar{u} = \overline{u_L},\ \overline{u'^2} = \overline{u_L'^2},\ C = C_L \quad \theta = \theta_L \tag{3.11}$$

$x > 0$, $y \rightarrow \infty$:

$$\bar{u} = \overline{u_L},\ \overline{u'^2} = \overline{u_L'^2},\quad C = C_L,\ \theta = \theta_L \tag{3.12}$$

$x > 0$, $y \rightarrow -\infty$:

$$\bar{u} = \overline{u_H},\ \overline{u'^2} = \overline{u_H'^2},\quad C = C_H,\ \theta = \theta_H \tag{3.13}$$

$x > 0$, $y = 0$:

$$\bar{u} = \overline{u_L} + \frac{\overline{u_H}-\overline{u_L}}{2},\ \overline{u'^2} = \overline{u_L'^2} + \frac{\overline{u_H'^2}-\overline{u_L'^2}}{2},\ C = C_L + \frac{C_H - C_L}{2},\ \theta = \theta_L + \frac{\theta_H - \theta_L}{2} \tag{3.14}$$

These boundary conditions lead to the following solutions (See Appendix A.2) to the proposed equations:

a. Equation of motion:

$$\frac{\bar{u} - \overline{u_L}}{\overline{u_H}-\overline{u_L}} = \frac{1}{2}\left[1 - \mathrm{erf}\left(\frac{y}{2}\sqrt{\frac{\overline{u_L}}{\nu x}}\right)\right] \tag{3.15}$$

b. Equation of turbulent energy:

$$\frac{\overline{u'^2}-\overline{u_L'^2}}{\overline{u_H'^2}-\overline{u_L'^2}} = \frac{1}{2}\left[1 - \mathrm{erf}\left(\frac{y}{2}\sqrt{\frac{\overline{u_L}}{\nu_t x}}\right)\right] \tag{3.16}$$

c. Equation of diffusion:

$$\frac{C - C_L}{C_H - C_L} = \frac{1}{2}\left[1 - \mathrm{erf}\left(\frac{y}{2}\sqrt{\frac{\overline{u_L}}{D_a x}}\right)\right] \tag{3.17}$$

d. Equation of energy:

$$\frac{\theta - \theta_L}{\theta_H - \theta_L} = \frac{1}{2}\left[1 - \mathrm{erf}\left(\frac{y}{2}\sqrt{\frac{\bar{u}_L}{\alpha_t\ x}}\right)\right] \qquad (3.18)$$

The above solutions contain the error function which is typical of solutions to the heat conduction equation. Several workers (Reichardt, 1944; Albertson, 1948; Liepmann and Laufer, 1947; Corrsin, 1943; Hinze, et al., 1948; Schlichting, 1960 and Forstall and Shapiro, 1950) have presented experimental results which confirm that velocity, temperature, and concentration distributions in jet boundaries and wakes can be represented by solutions containing error functions.

3.2 Turbulent Diffusion

A complete description of the transport in the model mixing region depends on an accurate determination of the air flow conditions. Since turbulence is the primary mechanism of concern, the statistical description introduced by Taylor (1921) offers the most accurate approach.

The following derivation of the fundamental equation of turbulent diffusion should apply to the model mixing region proposed in this investigation. For transport of the bacterial aerosol to occur in the model mixing region, the particles must move in a direction perpendicular to the opening (y-direction). The y-location of a given particle after a dispersion time of t would be:

$$y = \int_0^t v'(\xi)\, d\,\xi \tag{3.19}$$

where ξ represents the time lag between instantaneous velocity measurements. By computing the variance of the y-component of particle location:

$$\overline{y^2} = \overline{\left[\int_0^t v'(\xi)\, d\,\xi\right]^2} = \int_0^t \overline{v'(t)}\ \ \overline{v'(\xi)}\, d\xi \tag{3.20}$$

and consideration of the auto-correlation coefficient:

$$R(\xi) = \frac{\overline{v'(t)}\ \ \overline{v'(\xi)}}{\overline{v'^2}} \tag{3.21}$$

then:

$$\int_0^t \overline{v'(t)}\ \ \overline{v'(\xi)}\ d\xi = \overline{v'^2} \int_0^t R(\xi)\, d\xi \tag{3.22}$$

By integration of the left side of equation 3.22

$$\overline{v'(t)} \int_0^t \overline{v'(\xi)}\, d\xi = \overline{v'(t)}\ \overline{y} = \overline{v'^2} \int_0^t R(\xi)\, d\xi \tag{3.23}$$

By restating:

$$\overline{v'y} = \frac{1}{2}\ \frac{d}{dt}\left[\overline{y^2}\right] = \overline{v'^2} \int_0^t R(\xi)\, d\xi \tag{3.24}$$

then:

$$\overline{y^2} = 2\ \overline{v'^2} \int_0^T \int_0^t R(\xi)\, d\xi dt \tag{3.25}$$

which is the fundamental equation of turbulent diffusion first derived by Taylor (1921). This expression provides an accurate and direct method of determining the statistical dispersion of the bacterial aerosol through the opening into the low concentration air. This information is attainable by determination of a turbulent energy factor ($\overline{v'^2}$) and autocorrelation coefficients, both of which can be obtained by measurement of instantaneous velocity fluctuations.

3.3 Turbulent Transport Coefficient

The transport of the bacterial aerosol through the experimental opening will be presented as a turbulent transfer coefficient. This coefficient is based on Fick's law of diffusion (Treybal, 1955):

$$\frac{N_A}{A} = -D \frac{\partial C}{\partial y} \tag{3.26}$$

which describes the movement of some component due to a concentration gradient. The mass flux (N_A) represents the rate of movement and D is the proportionality constant or diffusion coefficient. When describing turbulent diffusion, such as in this investigation, the equation is written as:

$$\frac{N_A}{A} = -D_t \frac{\partial C}{\partial y} \tag{3.27}$$

where D_t is the eddy diffusivity.

The mixing region model and the corresponding transport of aerosol through an opening perpendicular to the concentration gradient, the variables of equation 3.27 can be separated in the following manner:

$$\frac{N_A}{A} \int_{o}^{b} dy = -D_t \int_{C_H}^{C_L} dC \qquad (3.28)$$

where b is equal to the width of the mixing region. By integration, equation 3.28 becomes:

$$\frac{N_A}{A} = \frac{D_t}{b} \; (C_H - C_L) \qquad (3.29)$$

with C_H and C_L being equal to the high and low concentrations, respectively, the ratio (D_t/b) can then be replaced by the transfer coefficient (k_c) in the following manner:

$$N_A = k_c \; A(C_H - C_L) \qquad (3.30)$$

This equation describes the turbulent transport coefficient to be used. One important factor must be recognized. Because of the entrainment mechanism involved in the model, this coefficient (k_c) will be proportional to the mixing region width and will not decrease as suggested in equation 3.29. However, the relationship of the coefficient to the mass flux (N_A), area (A) and concentration gradient $(C_H - C_L)$ remains. Therefore, the turbulent transfer coefficient (k_c) is excellent parameter to be measured experimentally in this investigation.

3.4 Eddy Diffusivity

Transport in the model mixing region occurs only due to turbulence as specified by basic assumptions in the description of the model. As indicated by equation 3.27, turbulent diffusion is described in terms of an eddy diffusivity D_t which is analogous to the diffusion coefficient in molecular diffusion. However, a basic difference does exist in that the molecular diffusivity is characteristic of the fluid in which diffusion occurs, whereas the eddy diffusivity is related more closely to the flow conditions which exist. Because of this difference, it will be necessary to determine an eddy diffusivity which corresponds to each set of flow conditions investigated.

The most desirable method for determining eddy diffusivities in the mixing region model would be by measurement of concentrations at points in the mixing region and use of equation 3.17. However, this approach is time consuming and would not provide the accuracy desired because of difficulties encountered in making point concentration measurements of bacterial aerosols. The statistical approach proposed by Taylor (1935) offers an alternative method. From the definition of the autocorrelation coefficient in equation 3.21, it is evident that the coefficient is unity at $\xi = 0$ and zero at $\xi \longrightarrow \infty$ Because of this relationship, it is possible to define some time (T) beyond which $R(\xi) = 0$. Then, it is possible to state equation 3.23 as:

$$\overline{yv'} = \overline{v'^2} \int_0^t R\ (\xi)\ d\xi \tag{3.31}$$

where $\overline{yv'}$ is constant for $t > T$ even though $\overline{y^2}$ is increasing continuously. For these conditions, the constant $(\overline{yv'})$ is defined as the eddy diffusivity:

$$D_t = \overline{v'^2} \int_0^t R(\xi)\ d\xi \tag{3.32}$$

which is constant for a given turbulent energy factor $(\overline{v'^2})$ and integral of the autocorrelation coefficient.

In addition, Taylor (1935) defines a "length scale of turbulence" as:

$$\ell_1 (\overline{v'^2})^{\frac{1}{2}} = \overline{v'^2} \int_0^t R(\xi)\ d\xi \tag{3.33}$$

or

$$\ell_1 = (\overline{v'^2})^{\frac{1}{2}} \int_0^t R(\xi)\ d\xi \tag{3.34}$$

This length scale is assumed to have the same relation to turbulent diffusion as the mean free path does in molecular diffusion. This value may provide considerable information on the mechanism of transfer for the mixing region model of this investigation.

3.5 Transport in the Mixing Region

For purposes of this investigation, transport of the bacterial aerosol from the high concentration region to the low concentration region will occur due to dispersion in the mixing region and entrainment on the low concentration side. Equation 3.25 describes the extent of dispersion in the direction perpendicular to the opening and $(\overline{y^2})^{\frac{1}{2}}$ should then represent the width of the mixing region on the low concentration side. The entrainment of the aerosol would occur due to the mean flow of air along the low concentration side.

If the dispersion time (t) is large compared to the time (T) required for $R(\xi) \rightarrow 0$, then equation 3.25 can be stated as:

$$\overline{y^2} = 2\overline{v'^2} \int_0^T R(\xi)\, d\xi \int_0^t dt = 2(\overline{v'^2})^{\frac{1}{2}}\, \ell_1 t \qquad (3.35)$$

For turbulence sufficient to maintain uniform aerosol concentrations, such as specified for in the mixing region model, dispersion time (t) should be large compared to the time (T). For each set of flow conditions, the apparent mixing region width can be defined as:

$$b = (\overline{y^2})^{\frac{1}{2}} = \left[2(\overline{v'^2})^{\frac{1}{2}}\, \ell_1 t\right]^{\frac{1}{2}} \qquad (3.36)$$

3.5a <u>Isovel-Isothermal Flow</u>

The first case to be analyzed will be that of equal flow through both sides of the mixing region model. The flux of bacterial aerosol can be evaluated by:

$$N_A = \int_0^b \bar{u}_L\, C\, dy \qquad (3.37)$$

where:

N_A = the number of aerosol particles passing through the opening per unit time.

b = the apparent width of the mixing region defined by equation 3.36.

$\bar{u}_L$ = mean velocity past the opening.

C = concentration of bacterial aerosol at any point in the mixing region.

By substitution of equation 3.17 into equation 3.37:

$$N_A = \frac{\bar{u}_L C_H}{2} \int_o^b \left[1 - \mathrm{erf}\left(\frac{y}{2} \sqrt{\frac{\bar{u}_L}{D_a \ x}} \right) dy \right] \tag{3.38}$$

where it is assumed that $C_L = 0$. From the definition of the turbulent transfer coefficient:

$$k_c = \frac{N_A}{C_H \ H} \tag{3.39}$$

and letting:

$$\beta = \frac{y}{2} \sqrt{\frac{\bar{u}_L}{D_a \ x}} \tag{3.40}$$

then:

$$k_c = \frac{\bar{u}_L}{2H} \int_o^b \mathrm{erfc} \ \beta \ dy \tag{3.41}$$

By rearrangement of the terms in equation 3.41, the equation can be stated in the following dimensionless form:

$$\frac{k_c D_t}{\overline{u'^2}\, b_o} = K' \frac{f(\beta)}{b_o} \frac{\overline{u_L} \nu_t}{\overline{u'^2}\, H} \frac{D_t}{\nu_t} \qquad (3.42)$$

where:

$$\frac{k_c D_t}{u'^2\, b_o} = \text{Dimensionless transport group} \qquad (3.43)$$

$$\frac{\overline{u_L} \nu_t}{\overline{u'^2}\, H} = \text{Dimensionless turbulence group} \qquad (3.44)$$

b_o = width of partition (3.45)

H = height of opening. (3.46)

$$f(\beta) = \int_o^b \text{erfc}\ \beta\ dy = \text{ierfc}(o) - \text{ierfc}\ (\beta) \qquad (3.47)$$

K' = experimental constant (3.48)

The entire transport of bacterial aerosol in the turbulent mixing region can be described by equation 3.42 when air flows are equal.

3.5b Turbulent Mixing with Unequal Velocities

The second case to be considered presents a more complex situation to analyze, since flow conditions and parameters vary across the mixing region. Since the dispersion length ($\overline{y^2}$) will vary across the mixing region, the mixing region width (b) as defined in equation 3.36 will vary, also. To define this parameter in a manner which will be representative of the actual situation, the measurement of dispersion ($\overline{y^2}$) obtained at the opening (y=o) will be used to define the mixing region width (b). The measurements obtained at this point should represent a mean of conditions which exist across the mixing region.

The mean velocity ($\overline{u}$) will vary across the mixing region, also. However, the region over which $\overline{u}$ varies before decreasing to $\overline{u}_L$ is small compared to the width of the mixing region (b) (See Appendix A.3). Therefore, the mean velocity ($\overline{u}_L$) can be used in equation 3.42 without introducing significant error.

3.5c Influence of Partition Width

In order to express results obtained with variable partition widths in the form of equation 3.42, some modification must be introduced. The influence of a wider partition at the initial point of mixing is to decrease the dispersion ($\overline{y^2}$) unless additional wake effects are introduced. For purposes of analysis, the mixing region width will be decreased by an amount equal to the partition width. The same expressions and relationships, as introduced previously, can then be used.

3.5d Turbulent Mixing with a Temperature Gradient

Since the proposed mixing region model for bacterial aerosol is based completely on turbulent transport, the influence of a temperature gradient across the opening is not taken into account. Two additional factors must be considered in this case: (a) the influence of temperature and relative humidity on viability of the aerosol and (b) the influence of a heat flux through the opening. By taking these factors into account, an expression similar to equation 3.42 can be used.

4. EXPERIMENTAL PROCEDURES AND EQUIPMENT

4.1 Equipment

In order to attain the specific objectives of this investigation, reasonable control of temperature and relative humidity was required. Therefore, all experiments were conducted in a room with an air temperature of 70° ± 3°F. and relative humidity of 70 ± 10%. Both the dew-point and dry-bulb temperatures were continuously recorded by a temperature recorder (Figure 4.1).

4.1a Aerosol Chamber

The overall interior dimensions of the aerosol chamber, shown schematically in Figure 4.2 were four feet by eight feet by four feet with a partition to divide it into two four foot cube compartments. The interior walls were constructed of 1/4 in. tempered masonite and the interior surfaces were finished with two coats of white enamel before polishing to a smooth finish. The partition contained an adjustable sheet metal section (Figure 4.3) which was two feet in width and could provide an opening of up to nine in. with the bottom of the opening 12 in. above the chamber floor.

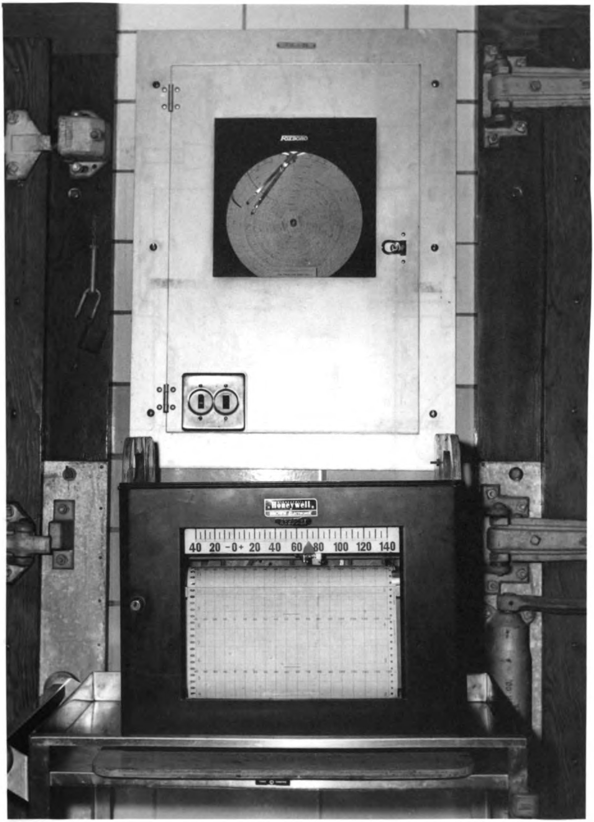

Figure 4.1.--Temperature and relative humidity recording instruments.

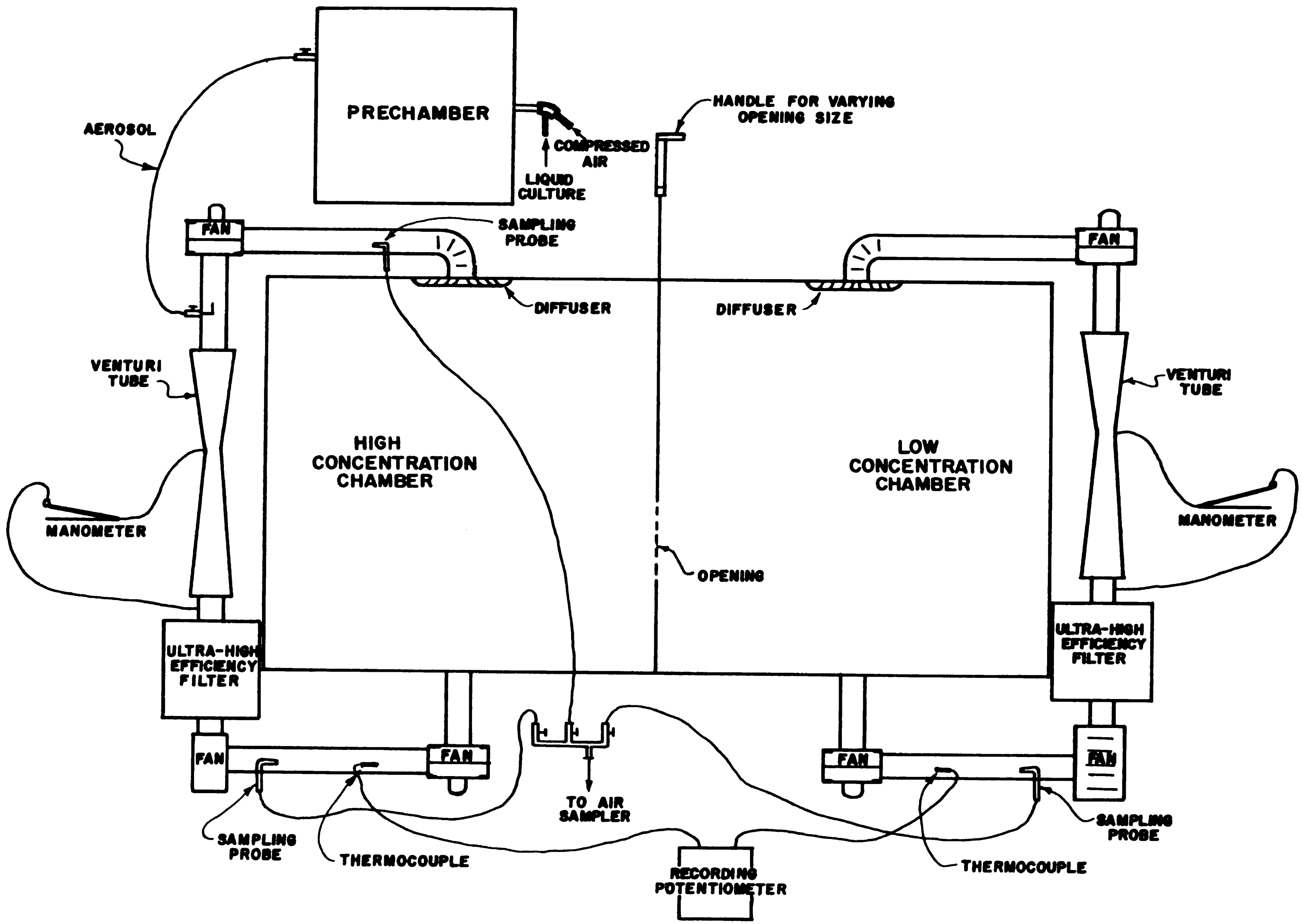

Figure 4.2.-- SCHEMATIC DIAGRAM OF AEROSOL CHAMBER AND RELATED INSTRUMENTATION

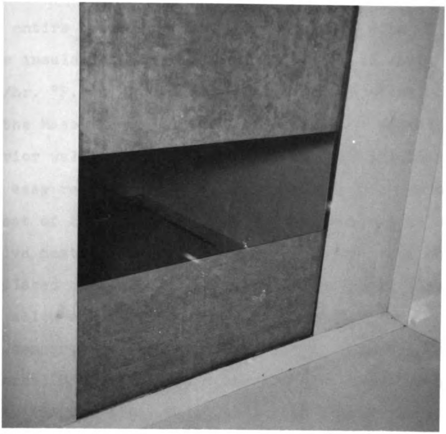

Figure 4.3.--Partition and opening between compartments of aerosol chamber.

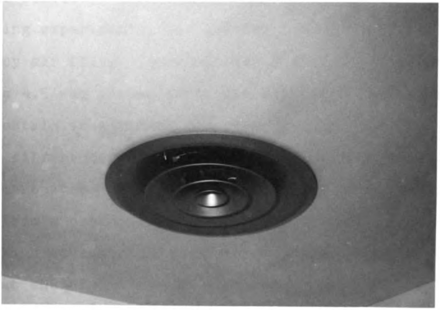

Figure 4.4.--Air diffuser in ceiling of one compartment of aerosol chamber.

The entire aerosol chamber was insulated with Microlite insulation material (density = 3/4 lb./ft.^{3}; k = 0.25 BTU/hr. °F. in.) which was placed in the space between the Masonite and 1/4-in. plywood which formed the exterior walls. The front of the chamber was designed to allow easy removal and was constructed of the same material as the rest of the chamber. Many experiments, which did not involve heating of the air, were conducted with the front replaced by two four foot sections of clear plexiglass to allow observation of the experiments.

The compartment interiors were mirror images. The only internal projections were the 11.5-in. diameter air diffusers, (Figure 4.4), which projected approximately one in. from the ceiling. The floor of each compartment contained the air outlet; a 3-in. diameter opening at the geometric center.

During experiments, air leaving the ultra-high efficiency air filter (American Air Filter Co.), shown in Figure 4.5 was passed through a venturi tube (Figure 4.6) to obtain an accurate measurement of air flow. Pressure differences in the venturi tube were measured by micromanometers (S.G., of fluid = 0.797). Bacterial aerosol from a prechamber was injected into the air stream and the high concentration air was uniformly distributed throughout the high concentration compartment of the chamber by an Anemostat CM1 air diffuser (Anemostat

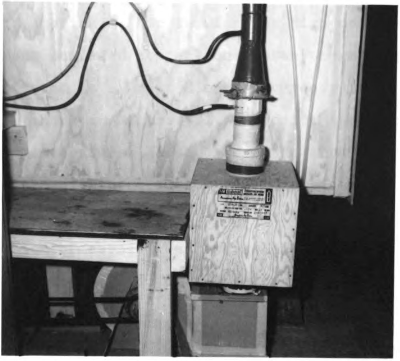

Figure 4.5.--Ultra-high efficiency air filter.

Figure 4.6.--Venturi tube and micromanometer used for air flow measurement.

Corporation of America). Air leaving the high concentration compartment passed a copper-constantan thermocouple, which was connected to a Brown Electronic recording potentiometer, shown in Figure 4.1 to provide a continuous record of air temperature. Just before the air passed through the ultra-high efficiency filter, air samples were collected by a Casella slit sampler (Figure 4.7) for determination of aerosol concentration. Air was sampled from the duct by vacuum through an isokinetic probe (Gelman Instrument Co.)

The low concentration compartment was equipped in a similar manner except that no aerosol was injected into the air stream and, in some experiments, the air was heated by a small resistance coil before entering the chamber. The 3-in. diameter duct serving the low concentration compartment was insulated with Microlite material to prevent heat loss during experiments involving heating of the air.

4.1b Aerosol Generation

The two primary parts of the aerosol generation system were the atomizer (DeVilbiss all glass No. 40) and the 24-in. cubical plexiglas prechamber shown in Figure 4.8. A clean regulated supply of compressed air was provided to the atomizer by a pressure regulator (C. A. Norgregn Co. Type 2A2) at a flow rate of 0.225 ft.^{3}/min. measured by a Brooks Rotameter Type 1110 flow meter

Figure 4.7.--Casella slit air sampler.

Figure 4.8.--Prechamber and related parts of aerosol generation system.

at 20 lb/in^2. Liquid culture was provided to the atomizer from a 2 liter aspirator bottle (Figure 4.9) used as a reservoir. A constant supply was provided by maintaining the proper level in the reservoir with respect to the atomizer. The liquid aerosol then passed into the pre-chamber where liquid portions of the droplets evaporated and larger particles settled to the floor. This method of aerosol generation was selected on the basis of investigations by Kethley, et al. (1956) which indicated that aerosol particles produced from 0.3% beef extract broth were consistently between 1.8 and 2.3 micron and not less than 90% of the particles carried single bacterial cells.

4.1c. Air Sampling

For most experiments, air was sampled at three ports consisting of Gelman isokinetic probes. The probes were connected to a common sampling station (Figure 4.10) by tygon tubing. The sampling station, which provided rapid consecutive sampling at various ports, was in turn connected to the Casella slit air sampler (Figure 4.7).

The Casella slit air sampler includes a vacuum source used to collect the samples at a rate of one ft^3 per min. The sampling method uses the solid impaction technique, which involves collection of all air-borne particles on a solidified agar surface. Air from the sampling probe

Figure 4.9.--Aerosol atomizer and culture reservoir.

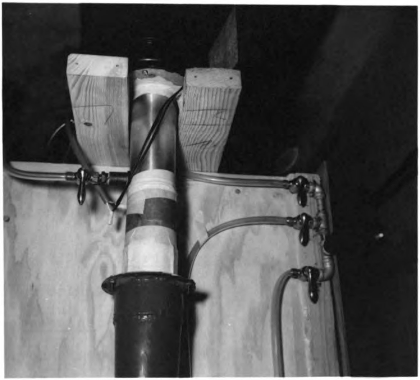

Figure 4.10.--Air sampling station and point of aerosol injection into duct.

passes through a 0.013 in. by one in. slit and particles are collected on the agar surface 2 mm below the slit. Since the petri dish, containing the agar media, is rotating continuously; the particles are distributed uniformly over the entire surface. Provisions for varying the sampling period to one, two or five min. are available.

4.1d Air Velocity and Turbulence

Mean air velocity and intensity of turbulence were measured using a constant current hot wire anemometer (Model HWB No. 216 by Flow Corporation, Arlington, Mass.). A 0.0005-in. diameter filament attached to a standard Flow Corporation probe was used for detection.

Figure 4.11 shows the hot wire anemometer and auxilary equipment used for turbulence measurement. The signal from the anemometer amplifier was fed through a 7 KC low pass filter to a Moseley X-Y recorder (Figure 4.12). The velocity fluctuations were recorded at settings of five volts/div. The Hickok Model 685 cathode ray oscilloscope was used for measurement of square-wave amplitudes required for calculation of air velocity fluctuation magnitudes.

4.2 Bacteriological Methods

The test organism used in this investigation was *Serratia marcescens*, which was selected on the basis of its natural occurrence, nonpathogenicity, simple nutritive requirements, production of a typical red colony,

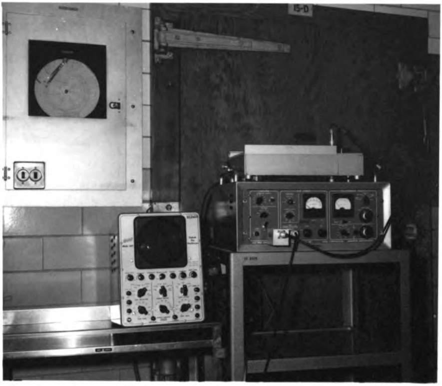

Figure 4.11.--Hot wire anemometer and auxilary equipment.

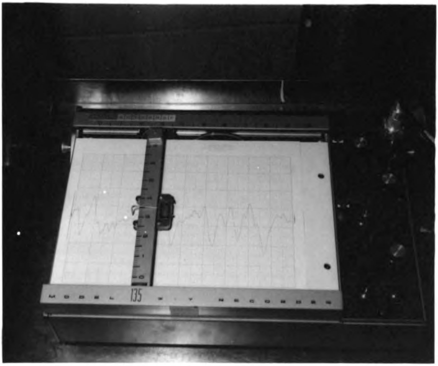

Figure 4.12.--X-Y recorder.

and the knowledge of its die-away characteristics at various temperatures and relative humidities (Kethley, et al., 1957).

4.2a Handling Techniques

Each week, new transfers of the test culture were started from the slant stock culture. The stock cultures were maintained in tryptone-glucose-extract (TGE) agar slant tubes, which were renewed at four to five week intervals to ensure that the culture was stable. The primary concern was to maintain the same variant of Serratia marcescens, since previous work by Kethley, et al. (1956) had indicated a loss in stability with formation of four variants with colonies of different colors. By maintaining and starting new stock cultures at the indicated intervals, the problem was kept to a minimum.

From the stock cultures, stored at 40° F., new transfers were started weekly into 60 ml. 0.3% beef extract broth and incubated at 32° C. Serial transfers were made into the same broth at 48 hr intervals. The broth culture was then used in an experiment after no less than three serial transfers.

4.2b Plating and Counting

The agar media used as a collection surface in the Casella slit air sampler was buffered, sodium chloride, TGE agar. This medium which consisted of 24 g TGE agar, five g sodium chloride, 2.5 g anhydrous dibasic sodium phosphate and 1000 ml water was proposed by Kethley, et al. (1956) in order to reduce incubation time. Colonies were counted with a Quebec counter after incubation of about 24 hr at 32°C.

4.3 Scope of Tests

The primary objective of the experiment was to determine all required values needed to complete the correlation of dimensionless groups presented in equation 3.42. In this relationship, the turbulent transfer coefficient (k_c) and eddy diffusivity (D_t) were of primary importance and were evaluated for various independent variables.

4.3a Turbulent Transfer Coefficient

The turbulent transfer coefficients (k_c) were evaluated according to equation 3.30. Values were obtained at various conditions in each of the following cases:

Opening size.--The opening between the two compartments of the aerosol chamber had a set width of two feet. However, turbulent transfer coefficients were determined at vertical heights (H) of three, six and nine in.

Air flow.--The air flow settings selected were done primarily on the basis of typical ventilation system values for number of air changes per hour. Turbulent transfer coefficients were determined for equal air flow through each compartment of the aerosol chamber for a range from 20 to 61 ft^3/min. These represent a range of approximately 20 to 60 air changes per hr.

Air flow difference.--Turbulent transfer coefficients were determined for various settings in order to evaluate the influence of an air flow rate difference between the two compartments of the aerosol chamber. Values were obtained at air flow rate difference intervals of ten ft^3 per minute up to a total difference of 40 ft^3 per min. Determinations were conducted with the flow rate difference in the same direction as the concentration gradient and also in the direction opposite the concentration gradient.

Geometry at initial mixing point.--The influence of geometry of the point where the two air streams in the two compartments join on the turbulent transfer coefficient was determined by varying the thickness of the partition between the two compartments. Experimental values were obtained for partition thicknesses of 0.0625, 0.3125, 0.5525 and 4.5 in.

Temperature gradient.--Turbulent transfer coefficients were determined for temperature gradients in the direction opposite the concentration gradient by heating the air in the low concentration compartment. The influence of a temperature gradient in the same direction as the concentration gradient was determined by heating the air in the high concentration compartment.

4.3b Eddy Diffusivities

Two approaches to determining eddy diffusivities were used as proposed in section 3.4. The values were determined for the same variations in independent variables as the turbulent transfer coefficient.

4.3c General Procedures

Evaluation of the turbulent transfer coefficient involved the establishment of a steady-state transfer through the opening between the two compartments. This was established by allowing the high concentration compartment to attain an equilibrium concentration (the concentration of the aerosol leaving the compartment was constant with time). Then by sampling the air at the outlet of the high and low concentration compartments, a steady-state flux of aerosol through the opening could be calculated. The calculation of the turbulent exchange coefficient followed based on the opening size and concentration gradient.

The losses of aerosol due to death, gravity, deposits, and transfer were calculated based on differences in concentration at the inlet and outlet of the high concentration compartment.

The determination of eddy diffusivities by the concentration profile through the opening involved the collection of air samples at 0.5 or 1 in. intervals across the opening.

Since values produced rather large fluctuations, several trials were involved in the establishment of a single diffusivity.

The measure of turbulence or velocity fluctuations with a hot wire anomometer (Flow Corp., 1958) to establish an eddy diffusivity involved the recording of the velocity fluctuation. This allowed establishment of a profile of the intensity of turbulence through the opening for various conditions. In addition, the calculation of the eddy diffusivity from the equation 3.22 was possible.

4.4 Analysis of Turbulence Data

The recording of instantaneous velocity fluctuations was used to determine the turbulent energy factor ($\overline{u'^2}$) and autocorrelation coefficient ($R(\xi)$) as outlined in section 3.2. The information obtained from each record was in terms of voltage which represented an air velocity:

$$u = \bar{u} + u' \tag{4.1}$$

A computer program to provide the desired information was developed.

Since:

$$\overline{u'^2} = \frac{1}{N} \sum u'^2 \tag{4.2}$$

then:

$$u^2 = (\bar{u} + u')^2 = \bar{u}^2 + 2\bar{u}\, u' + u'^2 \tag{4.3}$$

and:

$$\sum u^2 = \sum \overline{u}^2 + \sum u'^2 \tag{4.4}$$

since:

$$\sum u' = 0 \tag{4.5}$$

The turbulent energy factor would be defined as:

$$\overline{u'^2} = \frac{1}{N} \sum u^2 - \frac{1}{N} \sum \overline{u}^2 \tag{4.6}$$

and:

$$\sum u = \sum \overline{u} = \overline{u} \tag{4.7}$$

so:

$$\overline{u'^2} = \overline{u^2} - \overline{u}^2 \tag{4.8}$$

Equation 4.8 was programmed to provide the calculation of the turbulent energy factor ($\overline{u'^2}$). Values are presented in Table A-14.

The autocorrelation coefficient was defined in section 3.2 as:

$$R\ (\xi) = \frac{\overline{u'(t)}\ \overline{u'(t + \xi)}}{\overline{u'^2}} \tag{4.9}$$

In terms of equation (4.9), the product:

$$u'(t)\ u'(t + \xi) = [u(t) - \overline{u}]\ [u(t + \xi) - \overline{u}] \tag{4.10}$$

Then, the autocorrelation coefficient becomes:

$$R(\xi) = \frac{\overline{u(t)}\ \overline{u(t + \xi)} - \overline{u(t + \xi)}\ \overline{u} = \overline{u(t)}\ \overline{u} + \overline{u}^2}{\overline{u'^2}} \tag{4.11}$$

Equation 4.11 was programmed to calculate the autocorrelation coefficients presented in this investigation. The programs were calculated by the Michigan State University Control Data 3600 digital computer.

Analysis of data which required curve fitting was conducted by using a library program E2 UTEX LSCFWOP which approximated experimental data using the least squares method.

5. RESULTS AND DISCUSSION

5.1 Characteristics of the Aerosol Chamber

Preliminary tests were conducted to insure satisfactory operation of the aerosol chamber. This objective was attained by comparing performance of the chamber with a standard ventilation equation:

$$C = C_o \exp\left(-\frac{ft}{V}\right) \tag{2.6}$$

This equation has been used by Kethley, et al. (1957) to represent the dynamic emptying characteristics of an aerosol chamber and the establishment of equilibration times. The characteristics of one compartment of the chamber used in this investigation are illustrated in Figure 5.1. The data are somewhat scattered, but confirm the predicted expression. The standard error of estimate (SE_x) for agreement with the predicted line was ±0.831 min. The data are most widely dispersed when the chamber was nearly "empty" and approaching very low counts. Due to this fact, small variations in counts resulted in large variations in data presented.

According to Kethley, et al. (1957), verification of this equation indicates that the chamber is operating

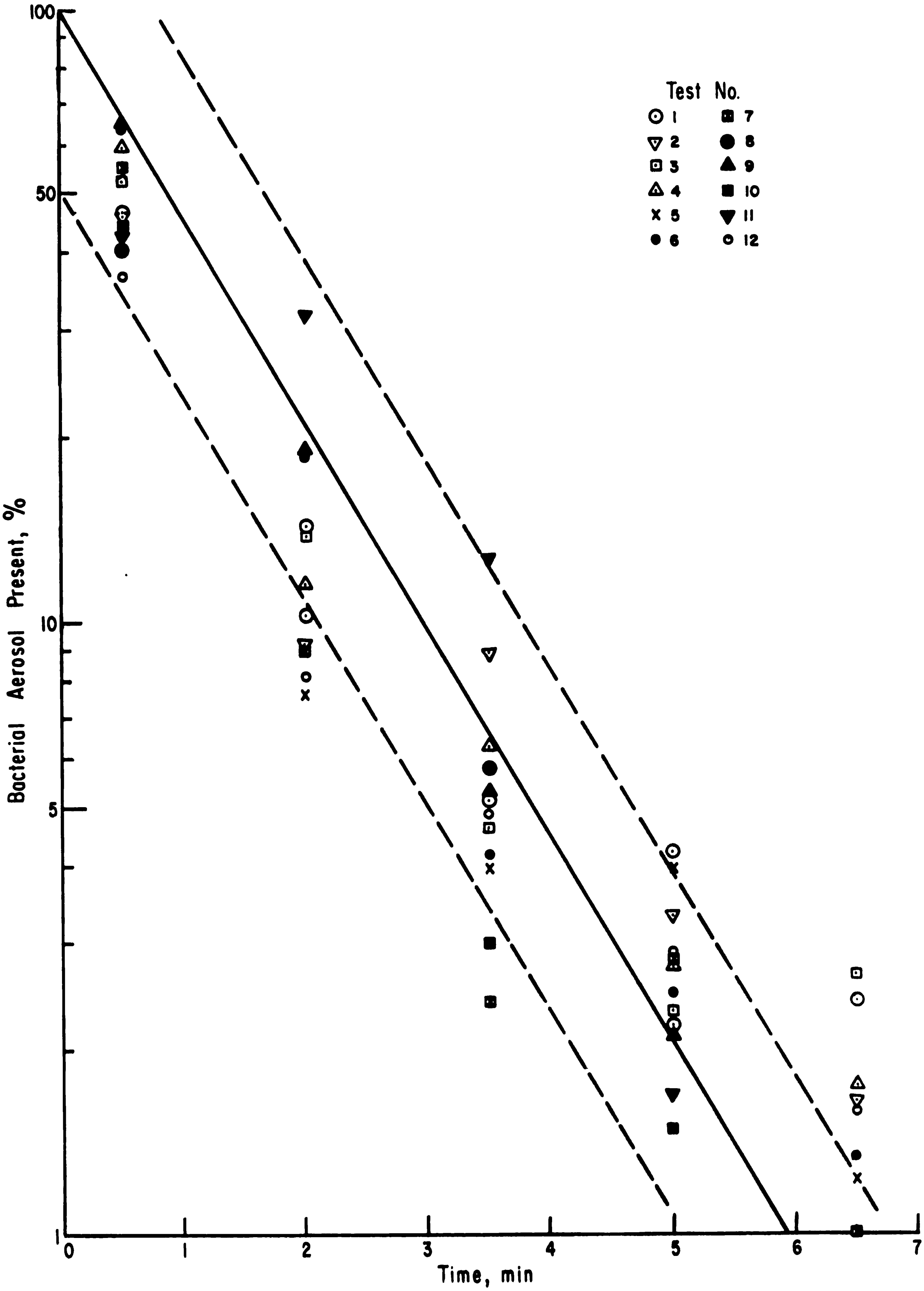

Figure 5.1.--Dynamic emptying characteristics of aerosol chamber.

effectively with bacterial aerosols. However, the physical meaning of the equilibration time requires further explanation. For the chamber in this investigation, the concentration of bacterial aerosol was increased to 99% or reduced to 1% (Figure 5.1) in 6 min. This equilibration time is generally accepted in aerosol liturature as the duration of time the aerosol is exposed to conditions in the chamber. For example, Kethley, et al. (1957) used this value as the time factor for calculation of death rate constants for air-borne bacteria. The validity of this usage may be somewhat questionable since not all of the aerosol particles may be exposed for exactly the equilibration time. The design of the chamber requires that sufficient turbulence be provided to maintain a uniform aerosol concentration. Therefore, the possibility of all particles passing through the chamber in the time indicated is questionable. Death rate constants based on this time factor must be recognized as average constants and their validity will depend on the uniformity of the aerosol with respect to particle size and characteristics.

In an attempt to obtain additional information on the characteristics of the chamber, air flow measurements were conducted at points throughout the chamber and primarily in the vicinity of the opening between the two compartments of the chamber. The first results of these measurements revealed that it was impossible to accurately measure a mean velocity with the hot wire anemometer. The reasons were two-fold: (a) mean velocities in the chamber were extremely low due to flow rates being used and (b) turbulent fluctuations of the velocity were very large compared to the expected mean velocity component. No further attempts to measure mean velocity were made and values used in calculations are based on the flow rate through the chamber and the cross-sectional area of the chamber. Mean velocities at each flow rate are presented in Appendix Table A-1. In addition, theoretical mean velocity profiles based on equation 3.9 are presented for conditions with different air flows through the two compartments.

Since turbulence was found to be a significant characteristic of the chamber, measurements to determine the turbulent motion were conducted. Using a hot wire anemometer and procedures described in section 4.4, several values describing the turbulence were obtained. From the variance of the instantaneous velocity fluctuations, it was possible to determine the turbulent energy factor ($\overline{u'^2}$) and the intensity of turbulence $\dfrac{\sqrt{\overline{u'^2}}}{\bar{u}}$. The variation of both of these parameters are plotted versus flow rate in Figure 5.2. Since the measurements were obtained where y = o and x = 9 in, it is evident that the intensity of turbulence, at this point, was not significantly affected by flow rate. However, the results

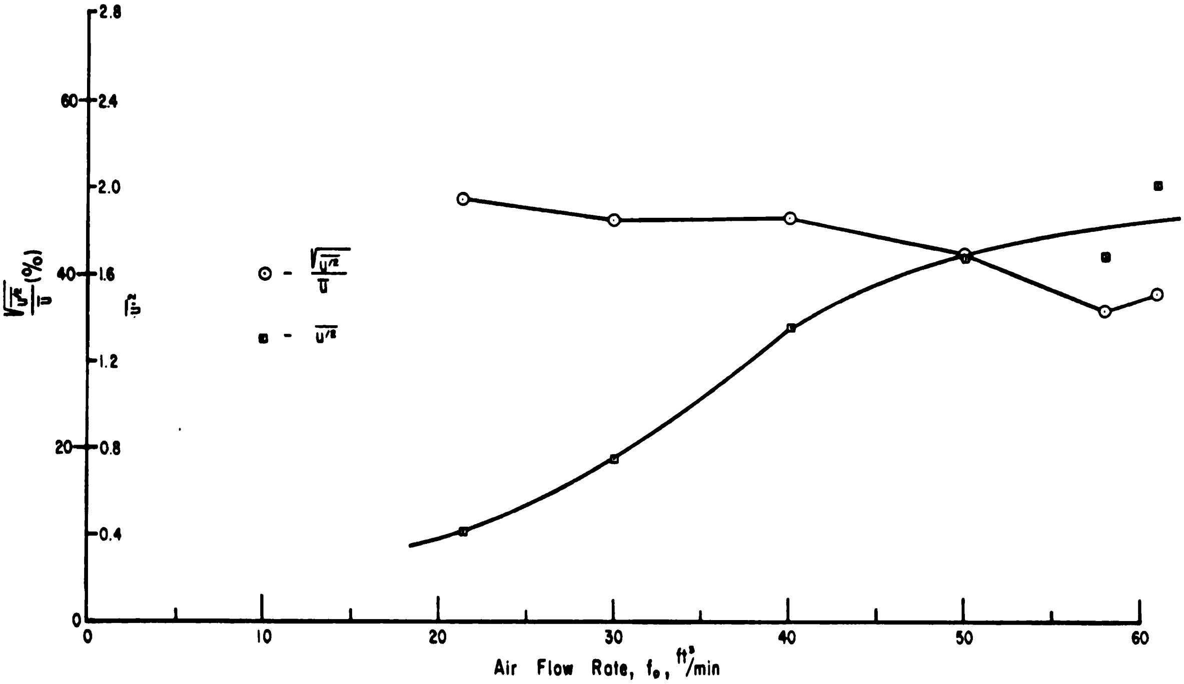

Figure 5.2.--Variation of turbulent energy and intensity of turbulence with air flow rate.

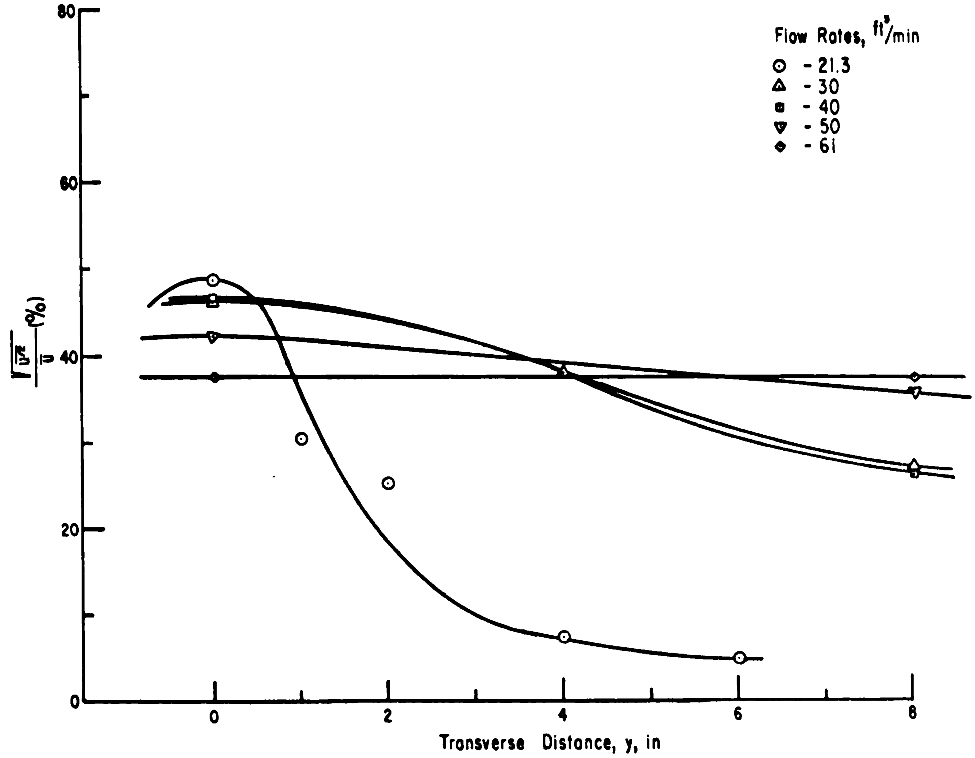

Figure 5.3.--Influence of transverse location on intensity of turbulence.

reveal that the turbulent energy factor increased steadily for the range of flow rates measured.

The influence of location on the intensity of turbulence is illustrated in Figure 5.3. The most obvious effect occurred with conditions of 21.3 ft^3/min of air through both compartments, where intensity of turbulence decreased rapidly with distance from the partition. This particular result clearly indicated a "wake effect" occurring due to the mixing of the two air streams at the opening. The influence of this factor becomes less evident when considering higher air flow rates. At flow rates of 30 and 40 ft^3/min, there was a significant decrease at a distance of 8 in. from the opening, while at flow rates of 50 and 61 ft^3/min, only slight decreases could be detected. The most logical explanation of these results is that the turbulence created by the diffusers in each of the compartments becomes greater with increasing flow rate. Apparently, air moving through the diffuser at around 20 to 25 ft^3/min remains in nearly laminar streams until mixing occurs at the opening. At the higher flow rates, the intensity of turbulence is higher throughout the chamber and the influence of the wake is not significant.

When an air flow gradient existed across the opening, the intensity of turbulence decreased in a rather uniform manner from the high flow rate to the low flow rate side.

In general, the partition width and opening height had no significant influence on intensity of turbulence.

5.2 Turbulent Diffusion

In order to describe the turbulent dispersion of an aerosol by the fundamental equation 3.20, two parameters are required: (a) the turbulent energy factor, and (b) the autocorrelation coefficient, $R(\xi)$.

5.2a Turbulent Energy

Although results presented in Figure 5.3 indicated that location did not influence the intensity of turbulence except at low flow rates, it is evident from Figure 5.4 that the influence of distance from the partition on the turbulent energy factor may be significant even at a flow rate of 50 ft^3/min. The change in the turbulent energy factor appears to be significant at all flow rates except 61 ft^3/min. However, the turbulent energy gradient probably does not contribute significantly to dispersion when compared to the turbulence mechanism and it may not be necessary to consider this except at the low flow rate (21.3 ft^3/min) where the gradient is very critical.

At a flow rate of 21.3 ft^3/min, the variation in the turbulent energy factor can be described by the equation:

$$\frac{\overline{u'^2} - \overline{u_L'^2}}{\overline{u_H'^2} - \overline{u_L'^2}} = \operatorname{erfc}\left(\frac{y}{2}\sqrt{\frac{\overline{u_L}}{\nu_t x}}\right) \qquad (5.1)$$

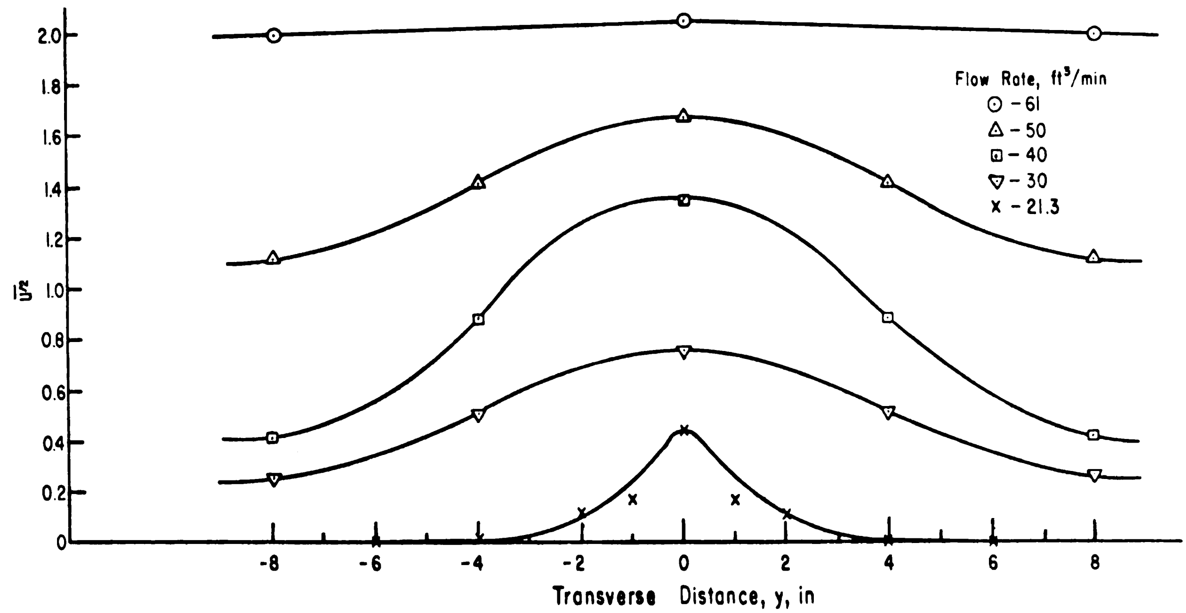

Figure 5.4.--Variation of turbulent energy in transverse direction.

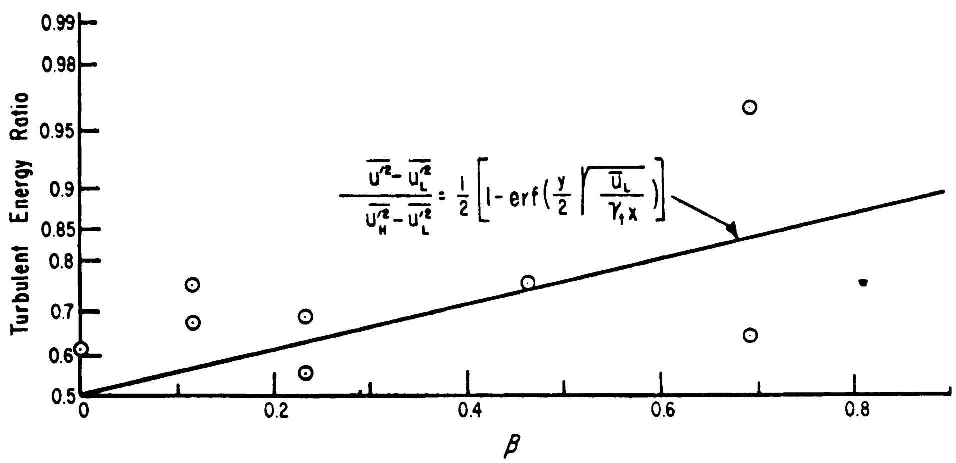

Figure 5.5.--Agreement of experimental data with equation 3.16.

which is the wake solution to equation 3.2. This equation should be very useful when describing transport at low air flow rates.

The change in the turbulent energy factor ($\overline{u'^2}$) across the mixing region between two different flow rates will be described by equation 3.16. This equation can be used to predict an apparent turbulent viscosity (ν_t) which is constant across the mixing region. The agreement of experimental data for the 50-20 air flow condition is illustrated in Figure 5.5. Since the results are presented on arithmetic probability coordinates, equation 3.16 is represented by the straight solid line shown. The agreement appears to be satisfactory for the limited data presented and produces a standard error of estimate (SE_y) of ±0.02424 for the turbulent energy ratio.

Using equation 3.16 and turbulent energy factor measurements obtained at the opening, turbulent energy profiles for various flow conditions are presented in Figures 5.6, 5.7 and 5.8. The three conditions illustrated in Figure 5.10 are for a flow rate of 70 ft^3/min on one side of the partition. As is evident, the turbulent energy profiles shift significantly to the low flow rate side as that flow rate is decreased from 50 to 30 ft^3/min. Similar profiles for flow rates of 60 and 50 ft^3/min on the high flow rate side of the partition are presented in Figures 5.7 and 5.8, respectively. In all cases, the

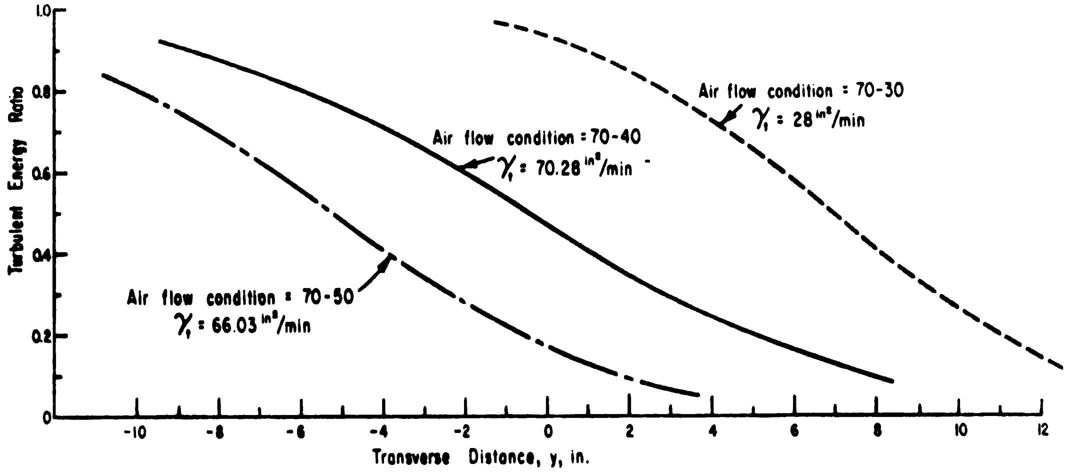

Figure 5.6.--Turbulent energy profiles with 70 ft^3/min. on high air flow rate side.

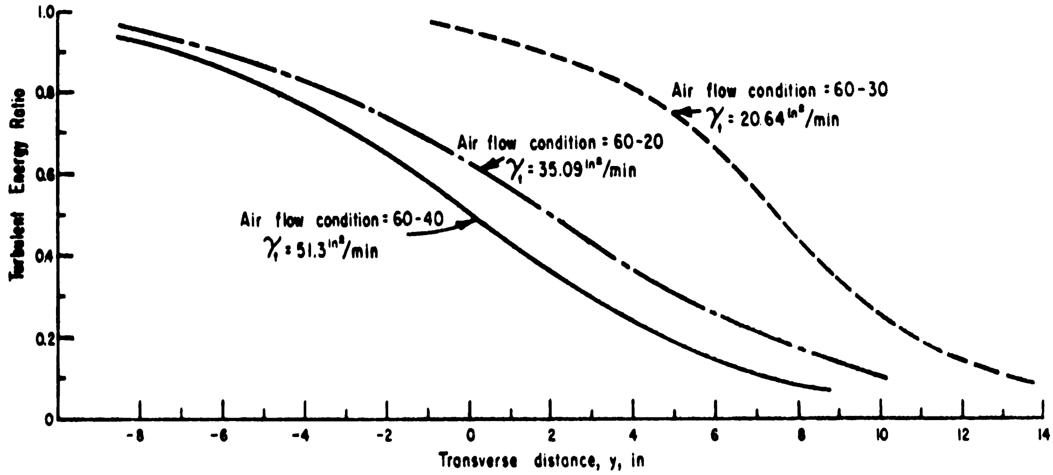

Figure 5.7.--Turbulent energy profiles with 60 ft^3/min on high air flow rate side.

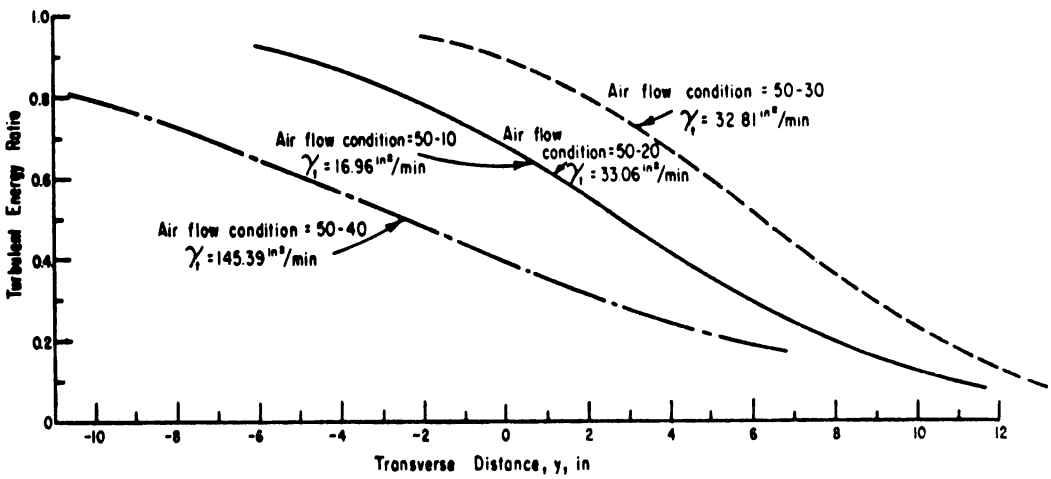

Figure 5.8.--Turbulent energy profiles with 50 ft^3/min. on high air flow rate side.

profile representing the minimum difference in flow rate is shifted toward the high flow rate side. One point of interest is that profiles shifted to the right have a common condition of 30 ft^3/min on the low flow rate side, while profiles from flow conditions with 20 or 10 ft^3/min are shifted to more central locations. An explanation of these results (Figures 5.6, 5.7 and 5.8) is not readily apparent. However, by reference to Figures 5.3 and 5.4, two factors were revealed: (a) the intensity of turbulence for 21.3 ft^3/min air flow at locations greater than 4 in. from the opening was very low (~5%) compared to values for an air flow of 30 ft^3/min and (b) the turbulent energy factor ($\overline{u'^2}$) for a flow rate of 21.3 ft^3/min approached zero at locations greater than 4 in. from the opening while the same value for 30 ft^3/min was significantly high even at 8 in. from the opening. The preceding observations indicate that two different types of mixing occur when the low air flow is 30 ft^3/min as compared to 21.3 ft^3/min. In the first case, both air flows are turbulent and contribute to turbulence in the mixing region. The gradual shift of the profiles to the right as the air flow difference increased exhibits an increase in momentum transfer as would be expected. In the second case, the mixing occurs between a turbulent air flow and a laminar air flow resulting in less turbulence in the mixing region. Although the momentum transfer may occur to even greater extent, it is not indicated by the profiles which illustrate turbulent energy ($\overline{u'^2}$) only.

5.2b <u>Autocorrelation Coefficients</u>

The second requirement for determination of dispersion of aerosol by turbulent diffusion is the autocorrelation coefficient $R(\xi)$ defined in equation 3.21. Using instantaneous velocity measurements obtained by procedures outlined in section 4.4 autocorrelation coefficients were calculated for 60 time lags (ξ) of 0.025 sec. Details on the computer program and procedures used are presented in section 4.4. A typical correlation curve for air flow in the experimental chamber is shown in Figure 5.9. The correlation curve decreases rapidly to negative values before damping to zero, as expected based on previous reports (Taylor, 1921; Frenkiel, 1953.) Data of this type were obtained at several locations and air flow conditions and all correlation curves were of the same general type. Some problems were encountered with complete damping to zero in many cases. This was attributed to the lag time becoming large compared to the overall sampling period. The influence of this factor on calculations to be presented is to produce values of somewhat larger magnitude. Both the dispersion factor ($\overline{y^2}$) and the eddy diffusivity (D_t) depend on the area under the correlation curve and lack of damping would cause this value to

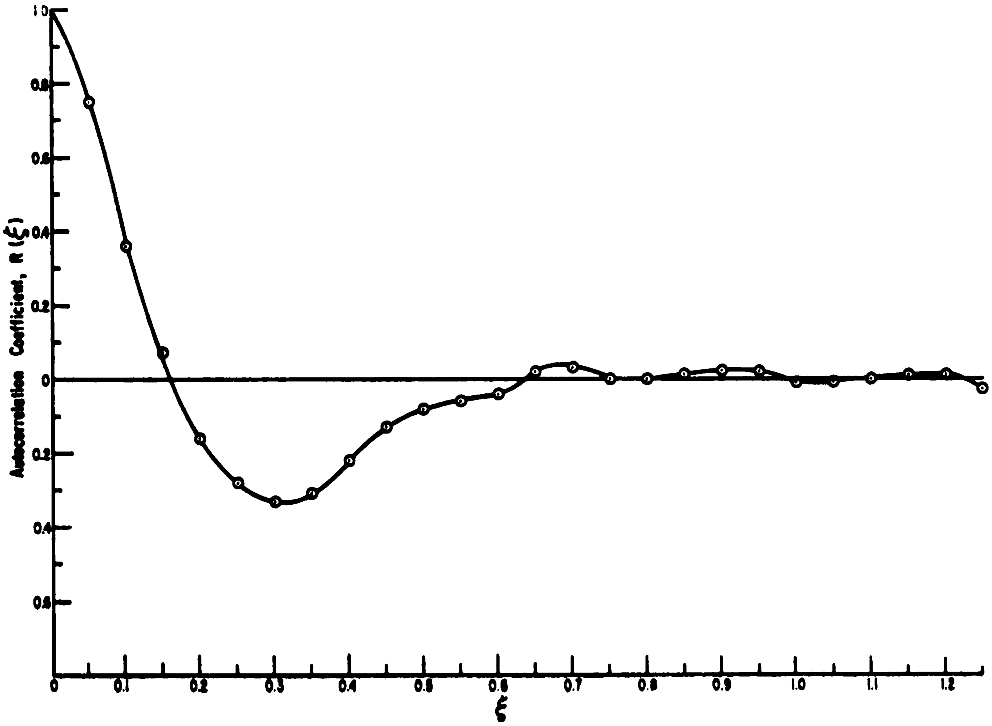

Figure 5.9.--Autocorrelation coefficients as influenced by time lag.

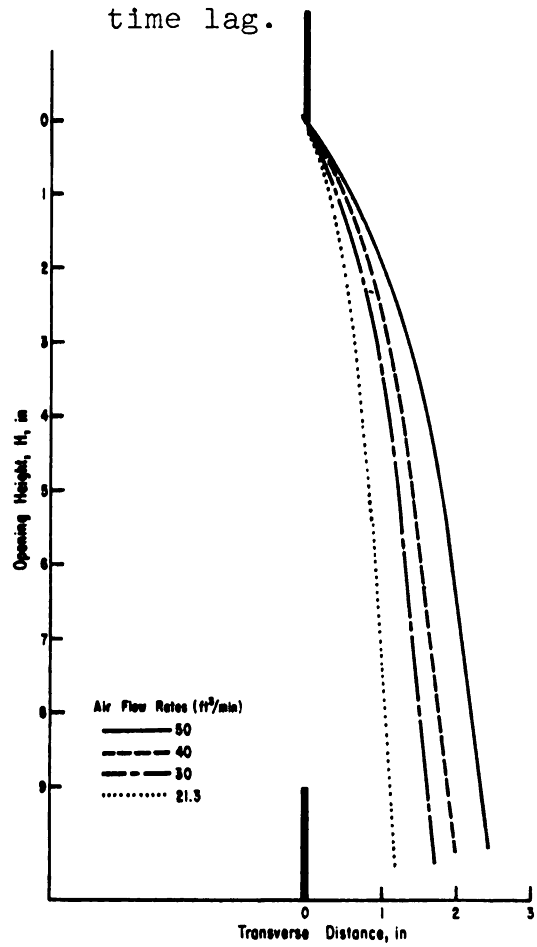

Figure 5.10.--Variations in apparent mixing region width with air flow and partition height.

TABLE 5.1a.--Summary of results.

Air Flow Rate High Conc.	Air Flow Rate Low Conc.	Air Flow Rate Diff.	Opening Height, H	Partition Width, b_o	Mixing Region Width, b	Transfer Coefficient	Eddy Diffusivity, D_t	$\frac{f(\beta)}{b_o}$	$\frac{\bar{u}_L \nu_t}{u'^2 H}$	$\frac{k_c D_t}{u'^2 b_o}$
(ft^3/min)	(ft^3/min)	(ft^3/min)	(in.)	(in.)	(in.)	[No./ft^2-min.(No./ft^3)]	($in.^2$/min)		($x10^{-3}$)	
61	61	0	9	0.0625	2.253	5.475	1.278	9.02	21.98	4.55
58	58	0	9	0.0625	2.023	5.431	0.984	9.02	19.66	4.24
50	50	0	9	0.0625	2.313	5.331	1.291	9.02	24.46	6.06
40	40	0	9	0.0625	1.833	5.126	0.560	9.02	13.16	3.89
30	30	0	9	0.0625	1.558	2.765	0.301	9.02	10.41	2.21
21.3	21.3	0	9	0.0625	1.064	0.818	0.106	9.02	6.19	0.55
50	60	-10	6	0.0625	1.908	5.424	1.060	9.03	34.94	4.85
50	50	0	6	0.0625	2.128	5.457	1.291	9.03	36.69	6.20
50	40	10	6	0.0625	1.248	5.325	0.330	9.03	14.60	2.99
50	30	20	6	0.0625	1.678	4.310	0.416	9.03	15.31	3.38
50	21.3	28.7	6	0.0625	1.948	2.518	0.388	9.03	12.12	2.20
50	10.7	39.3	6	0.0625	2.318	1.790	0.273	9.02	4.35	1.12
50	60	-10	3	0.0625	1.733	6.305	1.060	9.03	69.87	5.64
50	50	0	3	0.0625	1.943	8.989	1.291	9.03	73.38	10.21
50	40	10	3	0.0625	1.128	8.968	0.330	9.03	43.80	5.03
50	30	20	3	0.0625	1.528	5.620	0.416	9.03	45.93	4.41
50	21.3	28.7	3	0.0625	1.768	4.750	0.388	9.03	24.24	4.14
50	10.7	39.3	3	0.0625	2.128	2.780	0.273	9.03	8.70	1.74

TABLE 5.1b.--Summary of results.

Air Flow Rate High Conc.	Air Flow Rate Low Conc.	Air Flow Rate Diff.	Opening Height, H	Partition Width, b_o	Mixing Region Width, b	Transfer Coefficient	Eddy Diffusivity D_t	$\frac{f(\beta)}{b_o}$	$\frac{\bar{u}_L \nu_t}{u'^2 H}$	$\frac{k_c D_t}{u'^2 b_o}$
(ft^3/min)	(ft^3/min)	(ft^3/min)	(in.)	(in.)	(in.)	[No./ft^2-min.(No./ft^3)]	($in.^2$/min)		($x10^{-3}$)	
50	70	-20	9	0.0625	1.534	3.610	0.694	9.02	13.44	1.60
50	60	-10	9	0.0625	2.066	4.870	1.060	9.02	23.29	4.36
50	40	10	9	0.0625	1.352	4.190	0.330	9.02	9.73	2.35
50	30	20	9	0.0625	1.819	3.010	0.416	9.02	10.21	2.36
50	21.3	28.7	9	0.0625	2.101	1.795	0.388	9.02	8.08	1.57
50	10.7	39.3	9	0.0625	2.503	0.810	0.273	9.03	2.90	0.51
40	70	-30	9	0.0625	1.846	3.660	0.988	9.02	23.27	2.80
40	60	-20	9	0.0625	1.515	4.160	0.575	9.02	16.51	2.64
40	50	-10	9	0.0625	1.206	4.835	0.330	9.02	12.07	2.71
40	30	10	9	0.0625	1.369	4.390	0.238	9.02	11.34	3.82
40	21.3	18.7	9	0.0625	1.233	2.810	0.138	9.02	6.10	1.85
40	10.7	29.3	9	0.0625	2.189	1.320	0.210	9.02	4.01	1.14
30	70	-40	9	0.0625	1.880	3.890	0.278	9.02	25.43	2.27
30	60	-30	9	0.0625	1.934	4.470	0.256	9.02	28.56	4.90
30	50	-20	9	0.0625	1.396	5.130	0.210	9.03	16.89	4.03
30	40	-10	9	0.0625	1.178	4.870	0.238	9.02	15.12	4.24
30	21.3	8.7	9	0.0625	1.496	1.860	0.204	9.03	7.06	1.42
30	10.7	19.3	9	0.0625	1.828	0.935	0.150	9.02	4.38	0.88

TABLE 5.1c.--Summary of results.

Air Flow Rate		Air Flow Rate Diff.	Opening Height, H	Partition Width, b_o	Mixing Region Width, b	Transfer Coefficient	Eddy Diffusivity D_t	$\frac{f(\beta)}{b_o}$	$\frac{\bar{u}_L v_t}{u'^2 H}$	$\frac{k_c D_t}{u'^2 b_o}$
High Conc.	Low Conc.									
(ft^3/min)	(ft^3/min)	(ft^3/min)	(in.)	(in.)	(in.)	[No./ft^2-min. (No./ft^3)]	($in.^2$/min)		($x10^{-3}$)	
50	50	0	9	0.3125	2.063	6.026	1.291	1.80	24.46	1.37
40	40	0	9	0.3125	1.583	5.995	0.560	1.80	13.16	0.91
30	30	0	9	0.3125	1.308	4.066	0.301	1.80	10.41	0.65
50	60	-10	9	0.3125	1.816	4.674	1.060	1.80	23.29	0.84
50	40	10	9	0.3125	1.102	4.679	0.330	1.80	9.73	0.53
50	30	20	9	0.3125	1.569	3.143	0.416	1.80	10.21	0.49
50	21.3	28.7	9	0.3125	1.851	2.173	0.388	1.80	8.08	0.38
50	10.7	39.3	9	0.3125	2.253	0.665	0.273	1.80	2.90	0.09
50	50	0	9	0.5625	1.813	4.378	1.291	0.99	24.46	0.553
40	40	0	9	0.5625	1.233	4.132	0.560	0.99	13.16	0.348
30	30	0	9	0.5625	1.058	2.621	0.301	0.99	10.41	0.233
50	60	-10	9	0.5625	1.566	3.796	1.060	1.00	23.29	0.377
50	40	10	9	0.5625	0.852	3.466	0.330	0.98	9.73	0.216
50	30	20	9	0.5625	1.256	3.023	0.416	0.99	10.21	0.264
50	21.3	28.7	9	0.5625	1.574	1.699	0.388	1.00	8.08	0.165
50	10.7	39.3	9	0.5625	2.003	0.722	0.273	1.00	2.90	0.050

TABLE 5.1d.--Summary of results.

Temperature Gradient (°F.)	High Concentration Temperature, θ_{HC} (°F.)	Low Concentration Temperature, θ_{LC} (°F.)	Ratio θ_{HC}/θ_{LC}	Transfer Coefficient, k_c [No./ft^2-min (No./ft^2)]	$\frac{k_c\ D_t}{u'^2 b_0}$
-14	84.5	98.5	0.859	2.09	1.74
-12	80.5	92	0.875	2.30	1.91
-11	80	91	0.879	2.77	2.30
-10	80.5	90.5	0.890	2.99	2.48
- 5	78	83	0.940	4.10	3.41
0	75	75	1.0	5.22	4.34
5	83	78	1.063	6.33	5.26
10	90	80	1.125	7.44	6.18
12	94	82	1.147	7.89	6.55
12.5	94.5	82	1.152	8.02	6.66

be somewhat high. However, it is assumed that the area produced by lack of damping is small and, in addition, would be relatively consistent in all calculations.

The use of equations 3.25:

$$\overline{y^2} = 2\,\overline{u'^2} \int_0^T \int_0^t R(\xi)\, d\xi\, dt \qquad (3.25)$$

and 3.36:

$$b = (\overline{y^2})^{\frac{1}{2}} = [2(\overline{u'^2})^{\frac{1}{2}}\ell_{,}t]^{\frac{1}{2}} \qquad (3.36)$$

with $\overline{v'^2}$ replaced by $\overline{u'^2}$ (assumption e. in section 3), allows calculation of the statistical dispersion and an apparent mixing region width (b). As is evident from equation 3.36, the mixing region width is directly dependent on the dispersion time (t). The selection of a proper dispersion time for the aerosol moving from the high to the low concentration compartment of the aerosol chamber was not easy. The most likely selection appeared to be the equilibrium time discussed earlier in section 5.1. Since the dispersion did not start until the aerosol and filtered air came in contact at the initial point of mixing, aerosol moving from one side to the other was not exposed for the entire equilibration time. Calculations are based on dispersion times which are a fraction of the equilibration time. The fraction is based on the location of the initial point of mixing with respect to the overall height of the aerosol chamber. Using dispersion times (t) and equation

3.36, the apparent mixing region widths in Table 5.1 were calculated. The influence of air flow rate on the apparent mixing region width is illustrated in Figure 5.10. The results indicate that the width (b) increases with increasing flow rate. This relationship exists even though the dispersion time (t) increases significantly with decreasing flow rate.

In addition to statistical dispersion and apparent mixing region width, the autocorrelation coefficient is required in the calculation of the specific eddy diffusivity (D_t) according to equation 3.32:

$$D_t = \overline{u'^2} \int_0^t R(\xi)\, d\xi \qquad (3.32)$$

These values have been calculated for the required air flow situations and are presented in Table 5.1.

5.3 Concentration Distributions

In order to verify equation 3.17, which indicates that the concentration distribution in the mixing region should be described by some form of the error function, point concentration measurements were conducted in a limited number of situations. Measurements obtained permitted calculation of a single eddy diffusivity value at each point in the concentration profile. The values varied considerably; however, in order to satisfy equation 3.17, the apparent eddy diffusivity (D_a) must be constant. A mean of the values obtained in the concentration profile was used to present the data in Figure 5.11. Data obtained with flow conditions of 50 ft^3/min in the high concentration compartment and 50 ft^3/min and 30 ft^3/min in the low concentration compartment give good agreement with the proposed function.

The obvious weakness to the above method for determining eddy diffusivity values is lack of experimental accuracy for obtaining point concentration data. In addition, the function requires that the eddy diffusivity be constant in the mixing region which may or may not be true. Use of equation 3.22 allows calculation of specific eddy diffusivities (D_t) at points in the profile. Therefore, the values obtained by point concentration measurements will be referred to as apparent eddy diffusivities (D_a).

5.4 Transport of the Bacterial Aerosol

The complete description of the transport of a bacterial aerosol will combine two phases of study: (a) experimental determination of turbulent transfer coefficients (k_c) defined by equation 3.30 and (b) use of the dimensionless transport relationship presented in equation 3.42.

5.4a Experimental Transfer Coefficients

The influence of air flow rate on the experimental turbulent transfer coefficients (k_c) is illustrated in

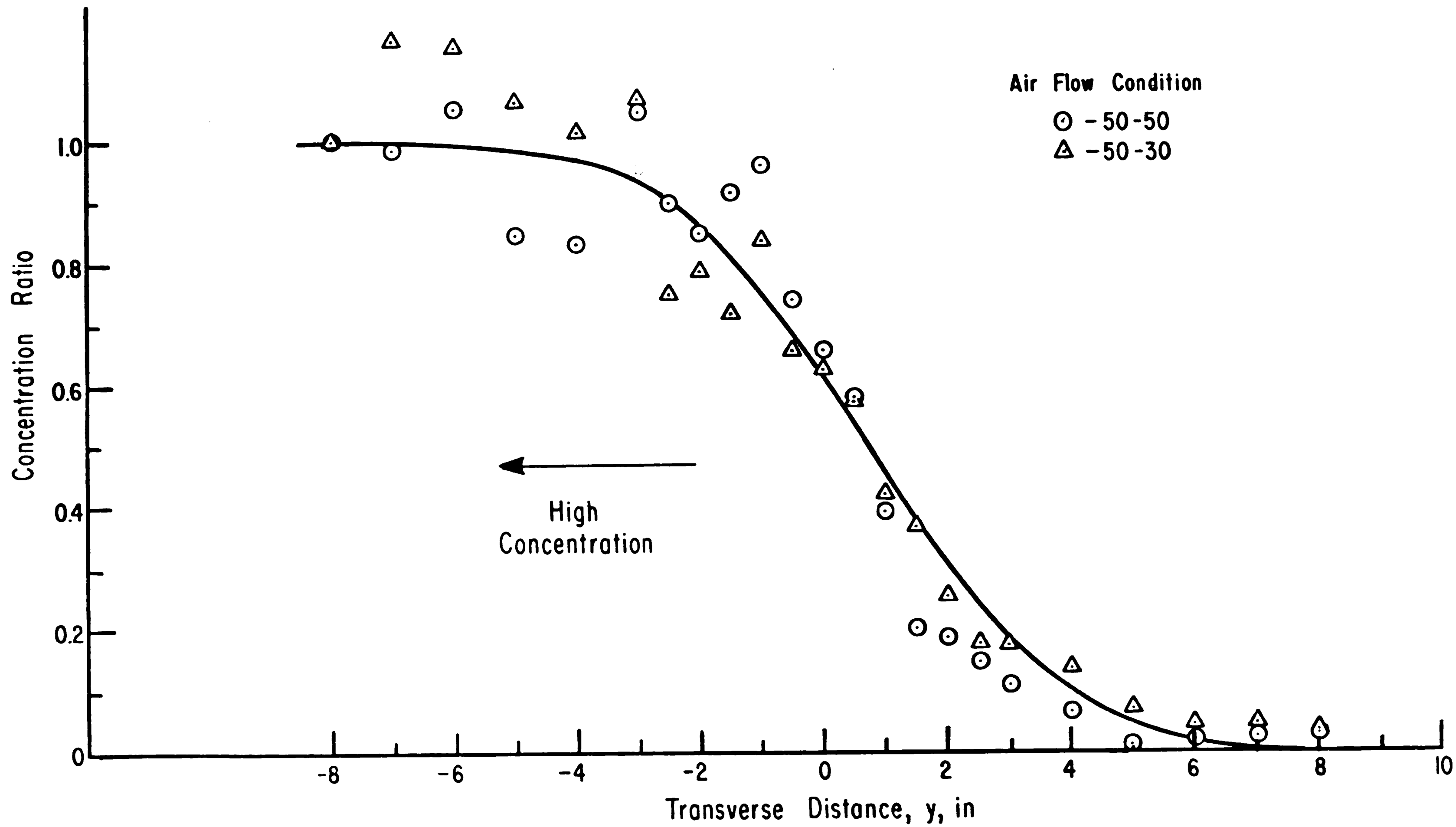

Figure 5.11.--Concentration distribution in mixing region.

Figure 5.12. The experimental data produced a coefficient of variation of ±0.176 for k_c from the curve selected according to procedures presented in section 4.4. As is evident, the coefficient (k_c) increases significantly between 20 and 40 ft^3/min, but becomes relatively constant above 40 ft^3/min.

Results (Figure 5.13) reveal the influence of air flow rate gradients on the turbulent transfer coefficient. For aerosol flow rates of 40 and 50 ft^3/min, the coefficient was maximum at equal flow rates. If the aerosol flow rate was 30 ft^3/min, the maximum transfer coefficient occurred between air flow gradients of -15 and -20 ft^3/min.

Figure 5.14 presents the relationship between a temperature gradient across the mixing region and the transfer coefficient (k_c). The correlation appears to be linear for the range of gradients investigated with a standard error of estimate (SE_y) of ±0.651 for experimental coefficients. The best fit curve for the experimental points can be described by the following equation:

$$k_c = 0.2195\ \Delta\theta + 5.09 \qquad (5.2)$$

Since the influence of a temperature gradient on transport of the bacterial aerosol in the mixing region could be related to several factors, an attempt was made to isolate a portion of the influence. Several investigators (Kethley, et al., 1956; DeOme, et al., 1944; Webb, 1959; Hayakaw and Poon, 1965) have determined and

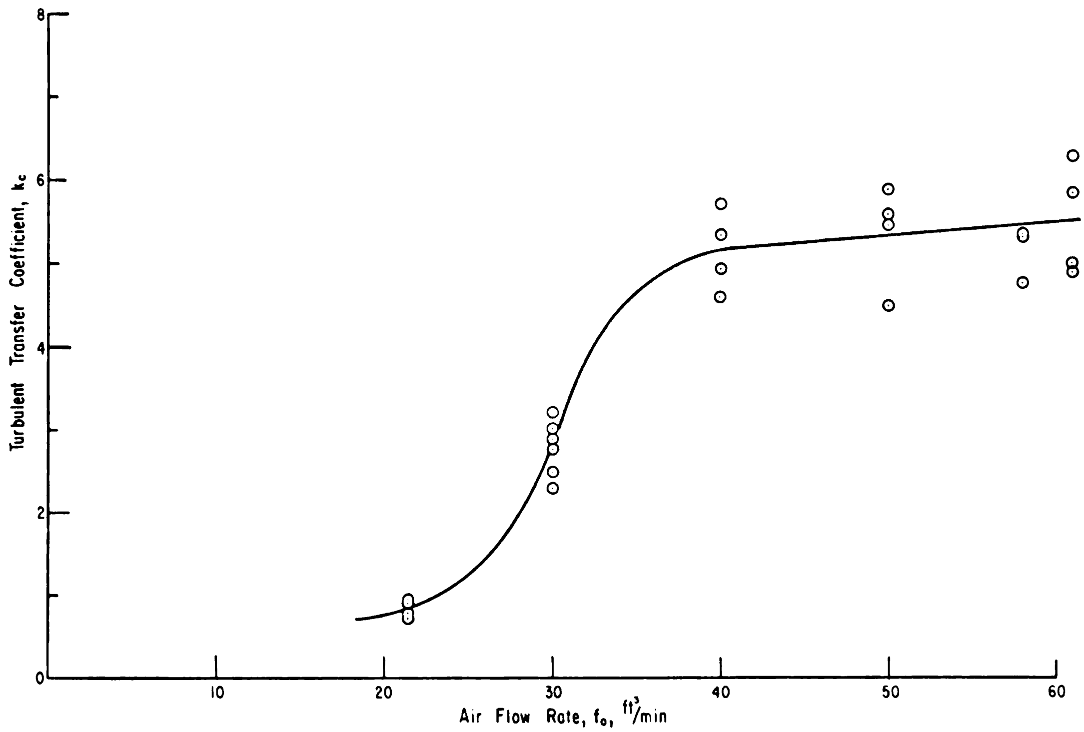

Figure 5.12.--Variation of transfer coefficient with air flow rate.

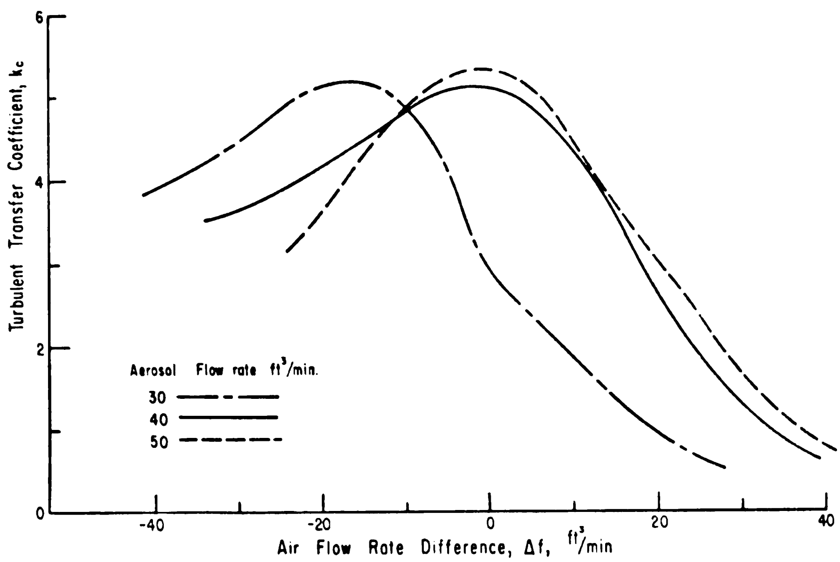

Figure 5.13.--Influence of air flow rate gradient on transfer coefficient.

discussed the influence of temperature and relative humidity on viability of bacterial aerosols. Since the temperature gradients maintained in the aerosol chamber were developed by heating the air, both factors could contribute to the relationship illustrated in Figure 5.14

Death rate constants for aerosols of Serratia marcescens were determined by Kethley, et al. (1956) for various temperatures and relative humidities. These data indicate the drastic influence of relative humidity along with the influence of temperature. However, experimental data were available only up to 80°F. while data of this investigation were obtained at temperatures as high as 98.5°F., therefore, extrapolation was required. In order to extrapolate the available death rate information as accurately as possible, the data were presented on semi-logrithmic coordinates as shown in Figure 5.15. Use of the $\log k_c$ versus $1/\theta_a$ relationship implies that the death of air-borne bacteria obeys a first-order kinetics reaction. This type of relationship has been used successfully by Webb (1959) and Hayakaw and Poon (1965). Results in Figure 5.15 indicate two stages of death, at least at lower relative humidities. The influence of temperature on death rate is small from 40° to about 70°F., but becomes very significant as the temperature increases above this level. The death rate

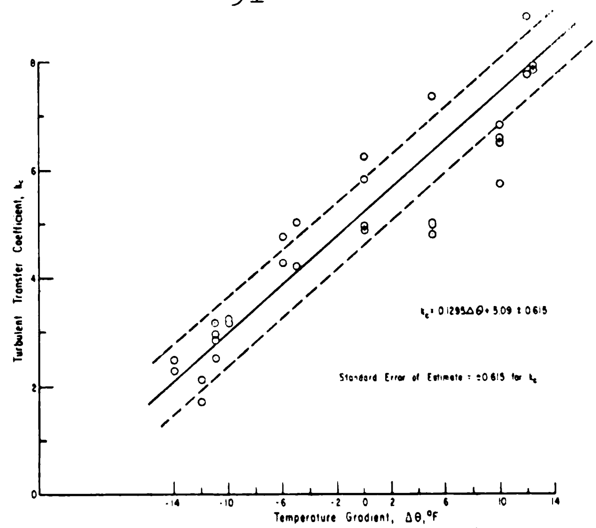

Figure 5.14.--Influence of temperature gradient on transfer coefficient.

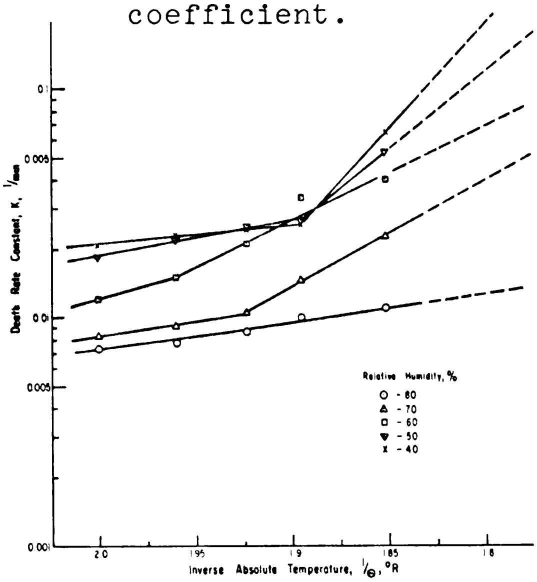

Figure 5.15.--Influence of temperature and relative humidity on death rate of <u>Serratia</u> <u>marcescens</u>.

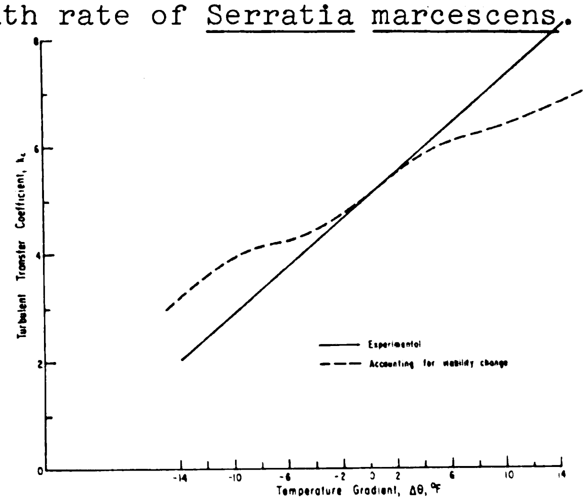

Figure 5.16.--Influence of aerosol viability on the relationship between temperature gradient and transfer coefficient.

constants used to account for viability changes due to the temperature gradient were obtained from Figure 5.15.

By adjusting the experimental turbulent transport coefficients to account for changes in viability during transport, the data illustrated in Figure 5.16 were obtained. The results reveal an increase in the coefficients (k_c) at negative temperature gradients and a decrease at positive temperature gradients. However, it is evident that viability does not account for the entire influence of the temperature gradient and other factors must be contributing to the apparent transport.

5.4b Dimensionless Relationships

In order to describe the transport of bacterial aerosols due to turbulent diffusion, dimensionless transport groups derived in section 3.5 will be used. The influence of each of the five basic parameters will be presented and discussed separately and then all data except that obtained for a temperature gradient will be used to establish an expression to describe the influence of all parameters.

The influence of dispersion time (t) and mean air velocity ($\bar{u}$) on dimensionless transport $\left(\frac{k_c' D_t}{\overline{u'^2} b_o} \Big/ \frac{f(\beta)}{b_o} \right)$ is illustrated in Figure 5.17. The results indicate an increase in transport with an increase in the dimensionless value ($\ell_1/\bar{u}t$) and reveals that the influence of the

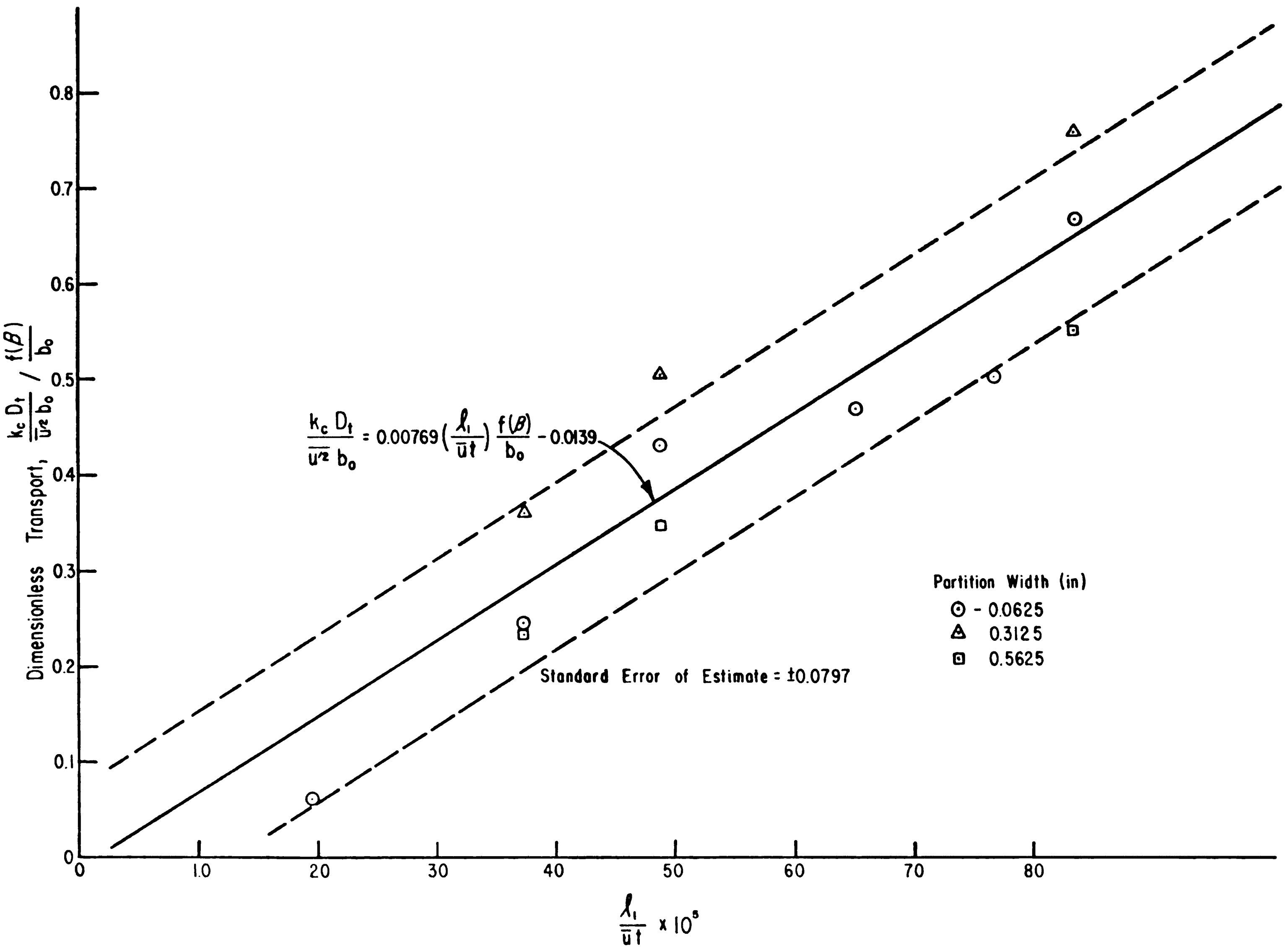

Figure 5.17.--Dimensionless transport as influenced by turbulence, dispersion time and mean air velocity.

length scale of turbulence (ℓ_1) dispersion time (t) overshadows that of the mean velocity ($\bar{u}$). The relationship is approximated very well by the equation:

$$\frac{k_c D_t}{\overline{u'^2} b_o} = 0.00796 \left(\frac{\ell_1}{\bar{u}t}\right) \frac{f(\beta)}{b_o} - 0.0139$$

for the three partition widths at the initial point of mixing. The standard error of estimate (SE_y) is ±0.0868 for the dimensionless transport group.

The influence of gradients in air flow between the two compartments of the aerosol chamber on the dimensionless transport group $\left(\frac{k_c D_t}{\overline{u'^2} b_o}\right)$ is presented in Figures 5.18, 5.19 and 5.20. For all three situations (50, 40 and 30 ft^3/min through the high concentration compartment), the transport decreases with an increasing positive air flow gradient. However, the influence of a negative gradient is not consistent. For f_o = 50 ft^3/min (Figure 5.18), the transport decreases with increasing negative air flow gradient in about the same manner as indicated for a positive gradient. The transport also decreases for small negative air flow gradients with f_o = 40 ft^3/min (Figure 5.19), but becomes relatively constant at a higher level than the positive gradient. When f_o was decreased to 30 ft^3/min, the transport increased with increasing negative air flow gradient before decreasing to a level nearly equal to that at equal air flow rates.

The transport characteristics illustrated in Figure 5.18, 5.19 and 5.20 are probably more closely related to turbulence in the mixing region than to the mangitude of the air flow gradient. This is clearly evident from Figure 5.20 where the dimensionless transport was low with equal flow rates of 30 ft^3/min. By increasing the flow in the low concentration compartment, the turbulence and transport both increased. This corresponding increase in both parameters continued until momentum transport from the low to the high concentration compartment was sufficient to overcome the increased transport due to turbulence. This same sequence of events did not occur at high air flow rates since turbulence levels were sufficiently high to produce nearly maximum transfer at equal flow rates. An increase in negative gradient did not increase turbulence enough to overcome the influence of increased momentum transfer. The increase in positive air flow gradient does not reflect an apparent influence of momentum transfer, indicating that the decreases resulted in significant decreases in turbulence.

Results (Figure 5.21) reveal the influence of partition width and apparent mixing region width on the dimensionless transport group. Several factors are illustrated by the results, however, most evident is the increase in transport with increasing partition width followed by a decrease to a level nearly equal to the transport with

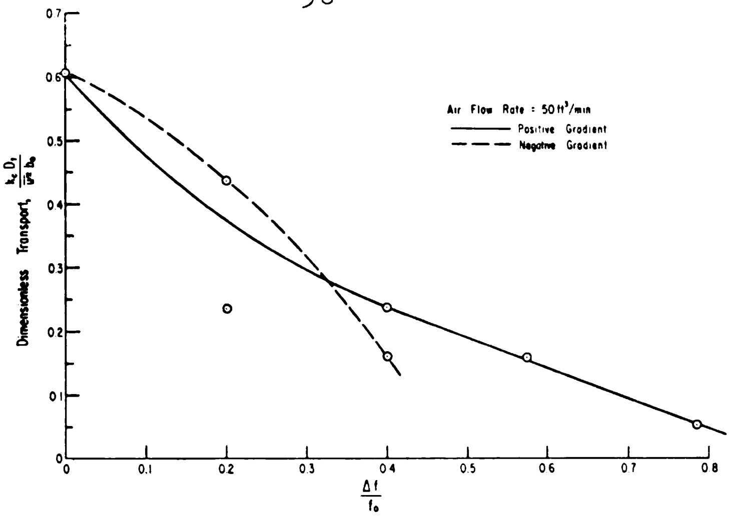

Figure 5.18.--Variation in dimensionless transport with air flow rate gradient for aerosol flow rate of 50 ft3/min.

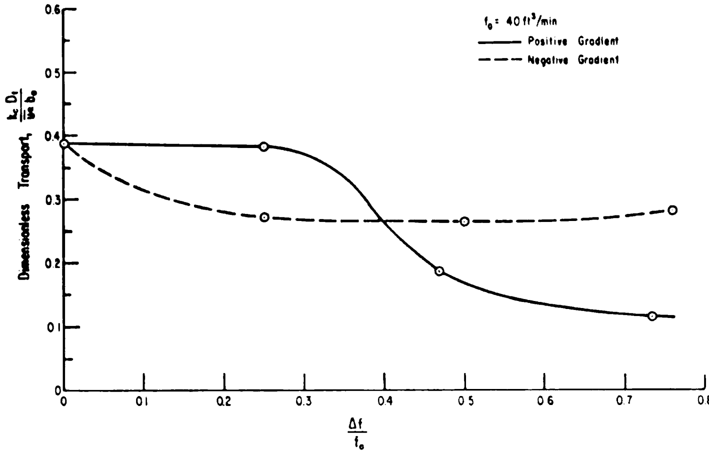

Figure 5.19.--Variation in dimensionless transport with air flow rate gradient for aerosol flow rate of 40 ft3/min.

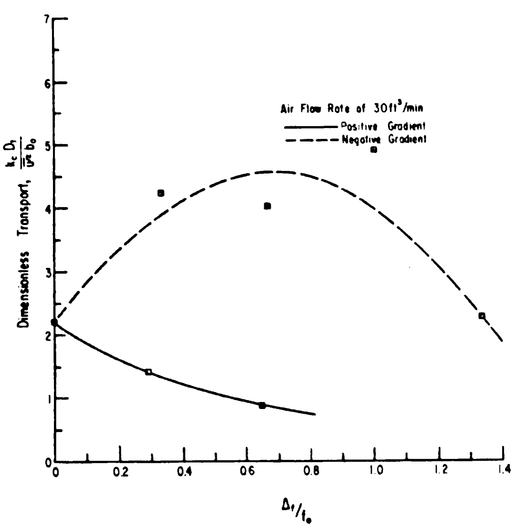

Figure 5.20.--Variation in dimensionless transport with air flow rate gradient for aerosol flow rate of 30 ft3/min.

the narrow partition. The increase detected must be due to increased turbulence in the mixing region even though it was not detected by measurements. It seems possible that small increases in turbulence could occur in the mixing region without detection and cause increased transport. The decreased transport with an even wider partition would be due to a significant decrease in the apparent mixing region width while turbulence may have increased only slightly.

The relationship between the dimensionless transport group $\left(\frac{k_c\ D_t}{u'^2\ b_o}\right)$ and dimensionless opening height (H/H') is presented in Figure 5.22. The decrease in transport per unit area with increasing opening height is apparent in all flow situations, but is most significant at equal flow rates. An explanation of this relationship is probably related to results presented in Figure 5.10 where the apparent mixing region width was shown to be a function of the square root of the distance from the initial point of mixing. Therefore, transport per unit area based on the dispersion-entrainment mechanism would larger for small openings.

The relationship between the dimensionless transport group $\left(\frac{k_c\ D_t}{u'^2 b_o}\right)$ and dimensionless temperature $(\theta_{HC}/\theta_{LC})$ based on the temperature gradient is presented in Figure 5.23

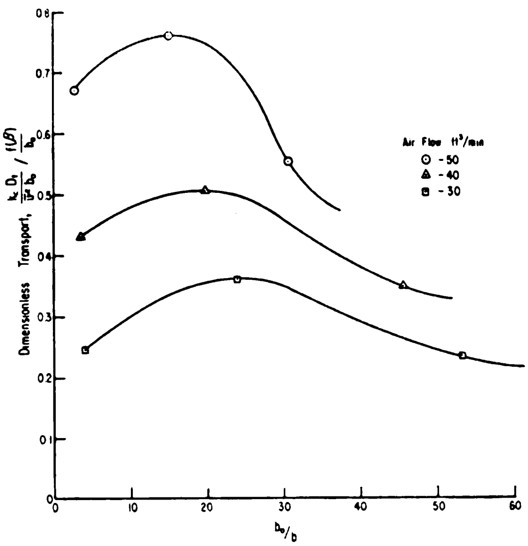

Figure 5.21.--Influence of partition width on dimensionless transport.

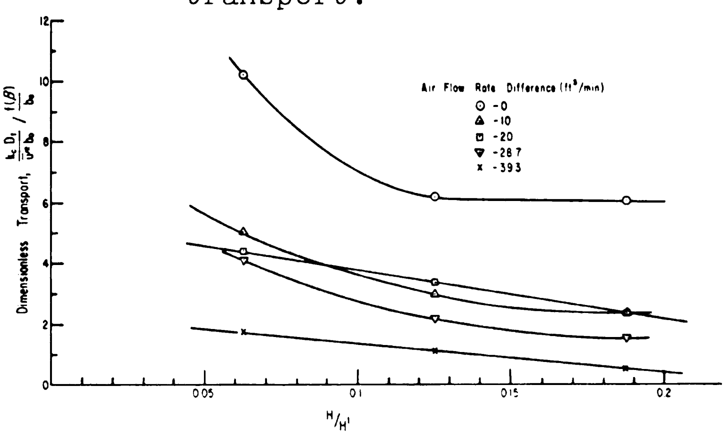

Figure 5.22.--Influence of opening height on dimensionless transport.

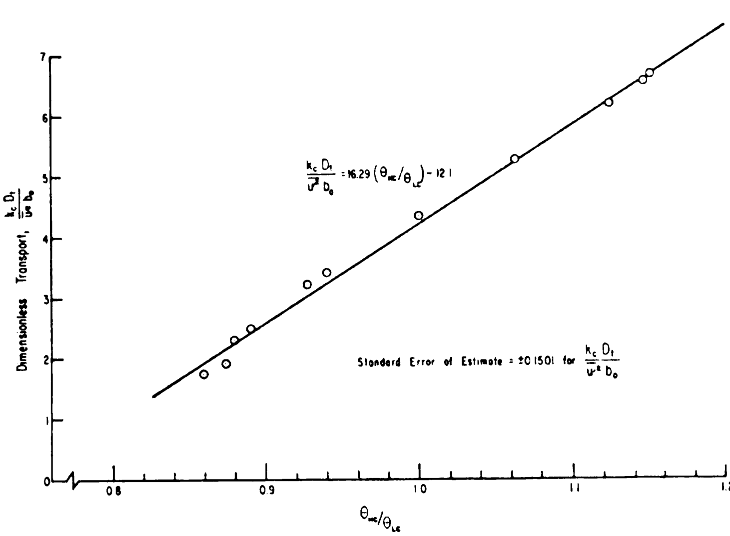

Figure 5.23.--Influence of dimensionless temperature ratio on dimensionless transport.

This relationship is very similar to the linear relationship presented earlier in Figure 5.14

$$\frac{k_c\, D_t}{\overline{u'^2} b_o} = 16.29\ (\theta_{HC}/\theta_{LC}) - 12.1 \qquad (5.4)$$

where θ_{HC} and θ_{LC} represent temperatures in the high and low concentration compartments respectively. An adequate explanation of the influence of temperature gradient other than the influence on viability is not apparent. A possible explanation is that convective heat transfer and a vapor pressure gradient across the mixing region contribute or decrease the transport of bacterial aerosol. The influence of these two factors would be in addition to the turbulent transport normally present.

The dimensionless transport equation derived in section 3.5 was:

$$\frac{k_c\, D_t}{\overline{u'^2} b_o} = K'\ \frac{f(\beta)}{b_o}\left(\frac{\overline{u_L}\ \nu_t}{\overline{u'^2}\ H}\right)\ \frac{D_t}{\nu_t} \qquad (3.42)$$

where K' represents a constant to be determined from experimental data. Using all data obtained without a temperature gradient, the slope of the straight line approximated by the least squares method was 0.01276. Therefore, K' = 0.01276 and equation 3.42 becomes:

$$\frac{k_c\, D_t}{\overline{u'^2} b_o} = 0.01276\ \frac{f(\beta)}{b_o}\left(\frac{\overline{u}_L\ \nu_t}{\overline{u'^2}\ H}\right)\ \frac{D_t}{\nu_t} + 0.772 \qquad (5.5)$$

Additional investigation indicated that data obtained with a temperature gradient could be described reasonably well by the same relationship by using the temperature ratio $(\theta_{HC}/\theta_{LC})$ as an exponent to the dimensionless transport group $\frac{\bar{u}_L \ \nu_t}{\overline{u'^2} \ H}$. This provides the following dimensionless relationship for data presented in Figure 5.24:

$$\frac{k_c \ D_t}{\overline{u'^2} b_o} = 0.01364 \ \frac{f(\beta)}{b_o} \left(\frac{\bar{u}_L \ \nu_t}{\overline{u'^2} \ H}\right)^{(\theta_{HC}/\theta_{LC})} \frac{D_t}{\nu_t} + 0.741 \qquad (5.6)$$

This relationship describes the transport of bacterial aerosols for all parameters studied in this investigation. The standard error of estimate (SE_y) of ± 1.004 for dimensionless transport values applied for a range of dimensionless turbulence values from 0 to 0.7.

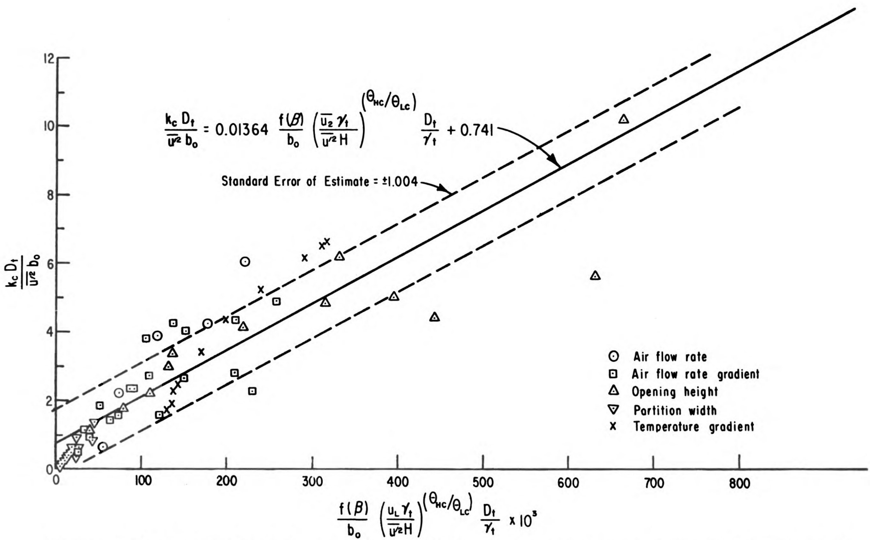

Figure 5.24.--Experimental correlation of dimensionless groups involved in bacterial aerosol transport.

6. SUMMARY AND CONCLUSIONS

1. By increasing the air flow rate gradient between two turbulent air streams, an increase in momentum transfer was indicated. A significant shift of the turbulent energy profiles to the lower flow rate side was revealed for rates of 30 ft^3/min or higher. At flow rates of less than 30 ft^3/min on the low flow rate side, an apparent decrease in momentum transfer resulted due to decreased turbulence in the mixing region.

2. Concentration distributions in the mixing region gave good agreement with the expression:

$$\frac{C - C_L}{C_H - C_L} = \frac{1}{2} \left[1 - \mathrm{erf}\left(\frac{y}{2} \sqrt{\frac{\bar{u}_L}{D_a\, x}} \right) \right]$$

where D_a is an apparent eddy diffusivity which is constant in the mixing region.

3. Transport of bacterial aerosol in a turbulent mixing region increased with increasing equal flow rates. The following relationship obtained from experimental data:

$$\frac{k_c\, D_t}{u'^2 b_o} = 0.00796 \left(\frac{\ell_1}{\bar{u}t} \right) \frac{f(\beta)}{b_o} - 0.0139$$

indicates that transport is a significant function of turbulence and dispersion time and is only slightly influenced by changes in mean air velocity.

4. At air flow rates above 30 ft^3/min, transport of bacterial aerosol was maximum at equal flow rates through both compartments of the aerosol chamber. At these flow rates, transport decreased with increasing positive or negative air flow rate gradients.

5. The width of partition at the initial point of mixing had only a slight influence on transport at air flow rates of 30 ft^3/min or higher. Transport increased at a partition width of 0.3125 in., but decreased as the width was increased to 0.5625 in. The decrease was attributed to a decrease in mixing region width corresponding to the increase in partition width.

6. Transport of bacterial aerosol decreased with increasing opening height. This was related directly to the apparent mixing region width, which was a function of the square root of the distance from the initial point of mixing.

7. A temperature gradient across the mixing region influenced transport of the bacterial aerosol as indicated by the expression:

$$\frac{k_c \; D_t}{\overline{u'^2} b_o} = 16.29 \; (\theta_{HC}/\theta_{LC}) - 12.1$$

which applies to a range of temperature gradients from -14° to +12.5°F.

8. The transport of a bacterial aerosol was described by the following dimensionless relationship, which considers all parameters studied:

$$\frac{k_\varepsilon D_t}{\overline{u'^2} b_o} = 0.01364 \frac{f(\beta)}{b_o} \left(\frac{\overline{u_L} \nu_t}{\overline{u'^2} H} \right)^{(\theta_{HC}/\theta_{LC})} \frac{D_t}{\nu_t} + 0.741$$

This relationship applies for dimensionless turbulence values between 0 and 0.7.

7. RECOMMENDATIONS FOR FUTURE WORK

The results of this investigation indicate the need for additional work in the following areas:

1. Investigation of turbulence levels and momentum transfer in mixing regions between laminar and turbulent air streams.
2. Additional investigation of transport mechanisms present in mixing regions formed by an air flow rate gradient.
3. Further investigation of mechanisms related to transport of bacterial aerosol in mixing regions as influenced by partition width at the initial point of mixing.
4. Investigation of bacterial aerosol transport with a temperature gradient across the mixing region.

APPENDIX

APPENDIX

A.1 Air Flow Measurement

From Eckman (1950), the following equation was used to calculate air flows through both compartments of the aerosol chamber:

$$q = \frac{\pi}{4} \; \frac{C_{VT} \; \beta^2 \; D^2}{\sqrt{1 - \beta^4}} \; \frac{\phi \; v_b}{M_b} \; \sqrt{\frac{M_1 (\nu_m - \nu_f)}{v_1}} \; \sqrt{2gh}$$

where:

q = air flow rate, ft^3/sec

C_{VT} = venturi discharge coefficient

β = diameter ratio = d/D

D = pipe diameter, ft.

ϕ = rational expansion ratio

v_b = specific volume of gas at base conditions, $ft^3/lb.$

M_b = moisture factor at base conditions

M_1 = moisture factor at upstream conditions

ν_m = weight density of manometer fluid, $lb./ft^3$

ν_f = density of fluid over manometer fluid, $lb./ft^3$

g = acceleration due to gravity, $ft/sec.^2$

h = manometer differential, ft.

Table A-1 shows the corresponding air flow rates and pressure drop values used in this investigation.

TABLE A-1--Pressure drop, air flow rate and mean air velocity

Pressure Drop (in. H_2O)	Air flow rate (ft^3/min)	Mean air velocity ($\bar{u}$) (ft/min)
0.018	10.7	0.667
0.074	21.3	1.333
0.260	40	2.500
0.410	50	3.120
0.550	58	3.625
0.600	60	3.750
0.610	61	3.813
0.800	70	4.375

A.2 Solution to Diffusion Equation

According to equation (3.8):

$$\bar{u} \frac{\partial C}{\partial x} = D_a \frac{\partial^2 C}{\partial y^2} \tag{A.1}$$

and boundary conditions (3.11), (3.12) and (3.14):

At $x = 0,\ y > 0:\quad C = C_L$ (A.2)

$x > 0,\ y = \infty:\quad C = C_L$ (A.3)

$x > 0,\ y = 0:\quad C = C_L + \dfrac{C_H - C_L}{2}$ (A.4)

The solution to equation (A.1) will be of the form:

$$C = f\ (\bar{u},\ D_a,\ x,\ y) \tag{A.5}$$

By use of linear relationships between variables, it is evident that:

$$C = A\ F\ \left(y\sqrt{\frac{\bar{u}}{D_a\ x}} \right) \tag{A.6}$$

By substitution of equation (A.6) into equation (A.1):

$$F''(\eta) = -\frac{\eta}{2}\,F'(\eta) \tag{A.7}$$

where:

$$\eta = y\sqrt{\frac{\bar{u}}{D_a x}} \tag{A.8}$$

By solving the differential equation (A.7):

$$F(\eta) = C = A \int_0^{\eta} \exp\,[-(\eta/2)\ ]\ d\eta + B \tag{A.9}$$

Since:

$$\frac{2}{\sqrt{\pi}} \int_0^{\eta} \exp[-\eta^2]\ d\eta\ . \tag{A.10}$$

is equal to the Gaussian error function, equation (A.9) can be expressed as:

$$C = A\ \mathrm{erf}\ \left(\frac{y}{2}\sqrt{\frac{\bar{u}}{D_a x}} \right) + B \tag{A.11}$$

Using the stated boundary conditions:

$$A = -\frac{C_H - C_L}{2}\ ; \quad B = C_L + \frac{C_H - C_L}{2} \tag{A.12}$$

So:

$$\frac{C - C_L}{C_H - C_L} = \frac{1}{2}\left[1 - \mathrm{erf}\ \left(\frac{y}{2}\sqrt{\frac{\bar{u}}{D_a x}} \right) \right] \tag{A.13}$$

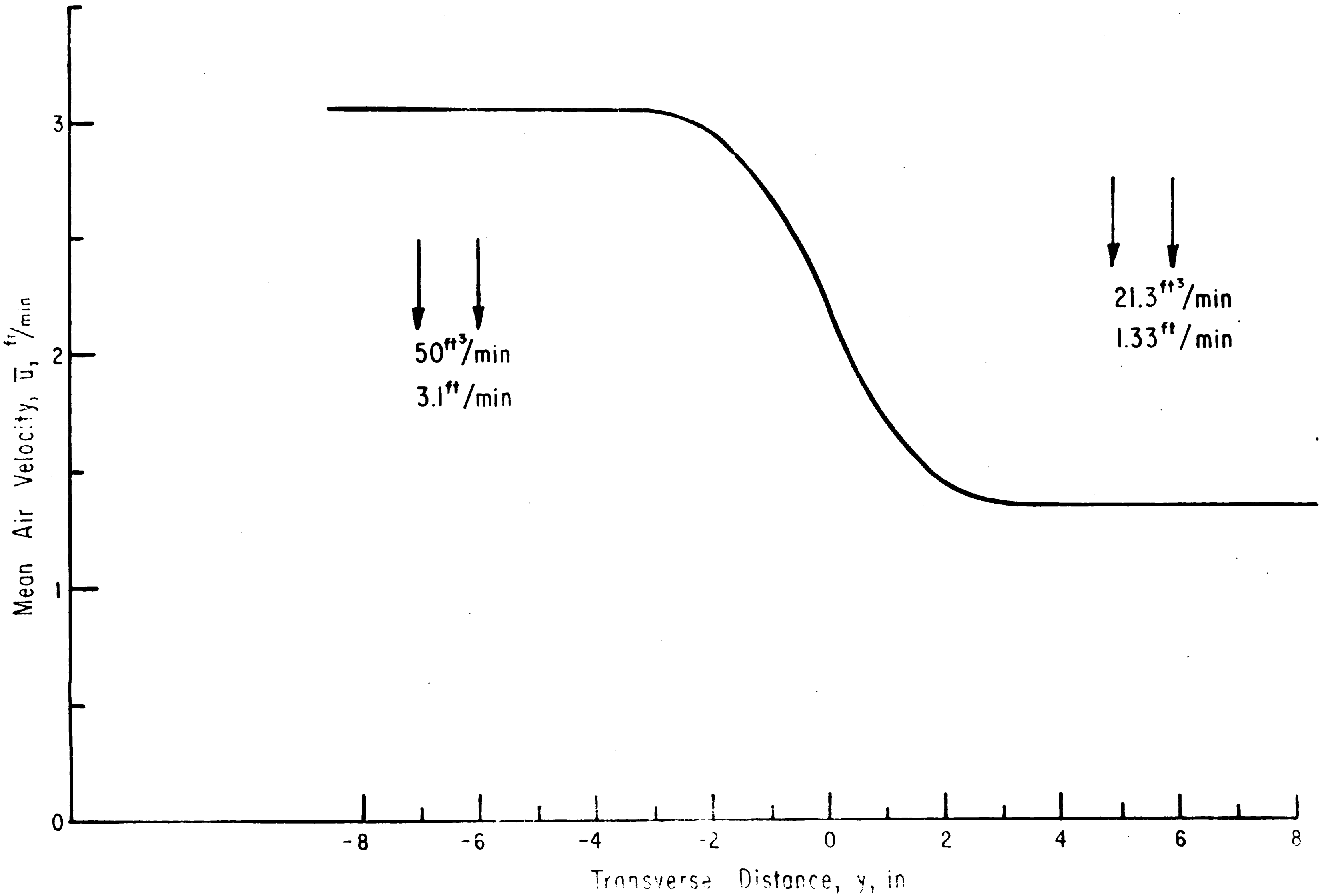

Figure A.1.--Mean air velocity profile.

A.3 Mean Air Velocity Profile

Using the solution to the equation of motion as presented in equation (3.15):

$$\frac{\bar{u} - \bar{u}_L}{\bar{u}_H - \bar{u}_L} = \frac{1}{2}\left[1 - \operatorname{erf} \quad \frac{y}{2}\sqrt{\frac{\bar{u}_L}{\nu x}}\right]$$

a predicted mean velocity profile can be obtained. The profile for the air flow conditions of 50 ft^3/min in one compartment and 21.3 ft^3/min in the other compartment of the aerosol chamber is present in Figure A.1.

A.4 Experimental Turbulent Transfer Coefficients

The data presented in Tables A.2 through A.13 represent individual trials conducted to determine the turbulent transfer coefficients (k_c) for various situations. From equation 3.30, it is evident that:

$$k_c = \frac{N_A}{A(C_H - C_L)} \qquad \text{(A.14)}$$

In the following tables, the steady-state transfer represents counts in air samples collected at the low concentration compartment outlet. The mass flux (N_A) was calculated from the mean of the steady-state values for flow rate in the low concentration compartment. The turbulent transfer coefficient was calculated from equation A.14.

TABLE A-2.--Influence of air flow rate on transport characteristics of air-borne bacteria with 1.5 ft^2 opening.

Air Flow Rate (ft^3/min.)	Steady-State Transfer (No./ft^3)	Mass Flux (No./min.)	Concentration Gradient (No./ft^3)	Transfer Coefficient [No./min-ft^2 (No./ft^3)]
61	22-21-25	1382.66	189	4.8771
	22-27-24	1484.33	170	5.8209
	24-22-25	1443.66	154	6.2496
	54-50-44	3009.33	405	4.9536
58	25-24-16	1256.67	157	5.3362
	42-34-27	1991.33	250	5.3102
	27-19-25	1372.66	221	4.1408
	35-31-33	1914.00	269	4.7435
50	54-47-50	2516.66	375	4.4741
	70-51-68	3150.00	387	5.4264
	36-40-38	1900.00	216	5.8642
	54-29-36	1983.00	238	5.5556
40	75-77-62	2853.33	358	5.3135
	87-65-67	2920.00	342	5.6920
	69-80-65	2853.33	415	4.5837
	77-63-79	2920.00	396	4.9158
30	28-38-31	969.99	283	2.2850
	37-37-26	999.99	242	2.7548
	61-61-58	1800.00	375	3.2000
	29-66-70	1650.00	382	2.8796
	43-38-42	1230.00	332	2.4699
	65-46-57	1680.00	373	3.0027
21.3	21-22-23	468.60	436	0.7165
	17-34-21	511.20	441	0.7728
	24-24-26	525.40	407	0.8606
	21-28-29	553.80	400	0.9230

TABLE A-3.--Influence of air flow rate gradient on transport characteristics of air-borne bacteria with 1.5 ft^2 opening and aerosol flow rate of 30 ft^3/min.

Air Flow Rate Difference (ft^3/min)	Steady-State Transfer (No./ft^3)	Mass Flux (No./min)	Concentration Gradient (No./ft^3)	Transfer Coefficient [No./min-ft^2 (No./ft^3)]
19.3	52-39-41	470.80	326	0.9628
	37-40-55	470.80	382	0.8216
8.7	36-39-43	837.80	261	2.1399
	40-40-43	873.30	308	1.8903
	28-20-20	482.80	187	1.7212
-10	49-54-58	2146.67	284	5.0391
	45-44-48	1826.67	220	5.5354
-20	57-46-62	2750.00	445	4.1199
	72-75-46	3216.67	482	4.4491
	32-27-34	1550.00	198	5.2189
	25-28-51	1900.00	205	6.1789
-30	42-39-30	2120.00	295	4.9717
	33-31-31	1900.00	277	4.5728
	73-78-80	4620.00	484	6.3636
	73-54-61	3759.99	432	5.8025
-40	40-38-26	2426.67	400	4.0444
	28-29-35	2146.67	369	3.8783

TABLE A-4.--Influence of air flow rate gradient on transport characteristics of air-borne bacteria with 1.5 ft^2 opening and aerosol flow rate of 40 ft^3/min.

Air Flow Rate Difference (ft^3.min.)	Steady-State Transfer (No./ft^3)	Mass Flux (No./min.)	Concentration Gradient (No./ft^3)	Transfer Coefficient [No./min-ft^2 (No./ft^3)]
29.3	48-53	540.35	323	1.1153
	63-64-65	684.80	307	1.4871
18.7	52-69-93	1519.40	357	2.8373
	60-67-92	1554.90	356	2.9118
10	89-91-88	2680.00	352	5.0758
	98-97-93	2880.00	431	4.4548
-10	38-37-35	1833.33	291	4.2001
	33-25-34	1533.33	263	3.8868
	24-30-27	1350.00	170	5.2941
	23-48-24	1416.67	168	5.6217
-20	39-30-34	2060.00	306	4.4880
	26-28-32	1720.00	262	4.3765
-30	40-39-37	2706.67	486	3.7129
	35-36-32	2403.33	446	3.5924

TABLE A-5.--Influence of air flow rate gradient on transport characteristics of air-borne bacteria with 1.5 ft^2 opening aerosol flow rate of 50 ft^3/min.

Air Flow Rate Difference (ft^3/min.)	Steady-State Transfer (No./ft^3)	Mass Flux (No./min.)	Concentration Gradient (No./ft^3)	Transfer Coefficient [No./min. ft^2 (No./ft^3)]
39.3	35-35-42	399.47	398	0.6691
	33-28-35	342.40	342	0.6675
	26-27-29	292.47	186	1.0483
	17-11-17	160.50	154	0.6948
28.7	38-39-43	852.00	255	2.2275
	38-44-37	844.89	207	2.7211
	92-60-53	1455.50	389	2.4944
	42-34-45	859.10	300	1.9091
20	56-68-63	1869.90	425	2.9333
	71-49-54	1740.00	403	2.8784
	31-34-39	1040.00	225	3.0815
10	31-23-27	1080.00	187	3.8503
	28-21-12	813.33	174	4.6743
	15-38-33	1013.30	191	3.5369
-10	50-58-48	3120.00	366	5.6831
	36-31-34	2020.00	303	4.4444
	30-32-28	1800.00	272	4.4118
-20	44-33-32	2543.33	447	3.7932
	29-29-34	2146.67	418	3.4237

TABLE A-6.--Influence of width at initial point of mixing on transport characteristics of air-borne bacteria at 50 ft^3/min.

Partition Width	Steady-State Transfer	Mass Flux	Concentration Gradient	Transfer Coefficient
(in.)	(No./ft^3)	(No./min.)	(No./ft^3)	[No./min-ft^2 (No./ft^3)]
0.3125	44-46-51	2350.00	272	5.7598
	47-35-41	2050.00	264	5.1768
	78-55-72	3416.67	321	7.0959
	65-60-34	2650.00	291	6.0710
0.5625	24-27-33	1400.00	253	3.6891
	33-26-38	1616.67	246	4.3812
	25-32-32	1483.33	209	4.7315
	40-27-36	1716.67	243	4.7097
	29-23-42	1566.67	308	3.3911
	43-52-47	2366.67	330	4.7811
4.5	53-59-51	2716.67	428	4.2316
	40-35-42	1950.00	350	3.7143
0.0625	54-47-50	2516.67	375	4.4741
	70-51-68	3150.00	387	5.4264
	36-40-38	1900.00	216	5.8642
	54-29-36	1983.00	238	5.5556

TABLE A-7.--Influence of width at initial point of mixing on transport characteristics of air-borne bacteria at 40 ft^3/min.

Partition Width (in.)	Steady-State Transfer ($No./ft^3$)	Mass Flux (No./min)	Concentration Gradient ($No./ft^3$)	Transfer Coefficient [$No./min-ft^2$ ($No./ft^3$)]
0.0625	75-77-62	2853.33	358	5.3135
	87-65-67	2920.00	342	5.6920
	69-80-65	2853.33	415	4.5837
	77-63-79	2920.00	396	4.9158
0.3125	57-40-42	1866.67	230	5.4106
	71-60-57	2506.67	254	6.5792
0.5625	58-44-51	2040.00	297	4.5791
	52-48-49	1986.67	284	4.6635
	53-30-47	1733.33	310	3.7276
	34-47-41	1626.67	305	3.5556
4.5	56-46-50	2026.67	297	4.5492
	70-57-55	2426.67	322	5.0242
	37-28-29	1253.33	267	3.1294
	32-41-43	1546.67	249	4.1410

TABLE A-8.--Influence of width at initial point of mixing on transport characteristics of air-borne bacteria at 30 ft^3/min.

Partition Width	Steady-State Transfer	Mass Flux	Concentration Gradient	Transfer Coefficient
(in.)	(No./ft^3)	(No./min.)	(No./ft^3)	[No./min-ft^2 (No./ft^3)]
0.0625	28-38-31	970.00	283	2.2850
	37-37-26	1000.00	242	2.7548
	61-61-58	1800.00	375	3.2000
	29-66-70	1650.00	382	2.8796
	43-38-42	1230.00	332	2.4699
	65-46-57	1680.00	373	3.0027
0.3125	50-59-66	1750.00	293	3.9818
	57-67-69	1930.00	310	4.1505
0.5625	46-44-38	1280.00	348	2.4521
	61-58-67	1860.00	437	2.8375
	50-39-36	1250.00	315	2.6455
	27-36-49	1120.00	293	2.5484
4.5	16-28-13	579.00	237	1.6287
	19-17-44	800.00	218	2.4465
	31-35-39	1050.00	323	2.1672
	27-44-40	1110.00	363	2.0386

TABLE A-9.--Influence of air flow rate gradient on transport characteristics of air-borne bacteria with 0.3125 in. partition.

Air Flow Rate Difference (ft^3/min.)	Steady-State Transfer (No./ft^3)	Mass Flux (No./min.)	Concentration Gradient (No./ft^3)	Transfer Coefficient [No./min-ft^2 (No./ft^3)]
39.3	15-12-19	164.07	158	0.6923
	11-9-10	107.00	134	0.5323
	75-67-85	809.63	669	0.8068
	56-48-42	520.73	551	0.6301
28.7	46-42-42	923.00	302	2.0375
	38-38-37	802.30	229	2.3357
	54-41-58	1086.30	415	1.7451
	79-98-54	1640.01	425	2.5726
20	26-27-15	680.00	144	3.1482
	25-38-33	960.00	204	3.1373
10	35-41-35	1560.00	197	5.2792
	96-78-92	680.00	544	4.3464
	101-117-116	3546.67	673	4.4114
0	44-46-51	2350.00	272	5.7598
	47-35-41	2050.00	264	5.1768
	78-55-72	3416.67	321	7.0959
	65-60-34	2650.00	291	6.0710
-10	10-13-11	680.00	97	4.6735

TABLE A-10.--Influence of air flow rate gradient on transport characteristics of air-borne bacteria with 0.5625 in. partition.

Air Flow Rate Difference (ft^3/min.)	Steady-State Transfer (No./ft^3)	Mass Flux (No./min.)	Concentration Gradient (No./ft^3)	Transfer Coefficient [No./min-ft^2 (No./ft^3)]
39.3	12-15-11	135.53	131	0.6897
	10-13-8-16	125.73	155	0.5408
	18-7-13	135.53	108	0.8366
	13-12-16	146.23	119	0.8192
28.7	25-18-21	454.40	178	1.7019
	21-26-20	475.70	187	1.6959
20	21-17-13	510.00	110	3.0909
	16-15-8	390.00	88	2.9545
10	37-28-28	1240.00	216	3.8272
	23-14-15	693.33	137	3.3739
	23-16-16	733.33	153	3.1954
0	24-27-33	1400.00	253	3.6891
	33-26-38	1616.67	246	4.3812
	25-32-32	1483.33	209	4.7315
	40-27-36	1716.67	243	4.7097
	29-23-42	1566.67	308	3.3911
	43-52-47	2366.67	330	4.7811
-10	31-18-19	1360.00	214	4.2368
	16-17-14	940.00	171	3.6647
	13-9-12	680.00	130	3.4872

TABLE A-11.--Influence of air flow rate gradient on transport characteristics of air-borne bacteria with 1.0 ft^2 opening.

Air Flow Rate Difference	Steady-State Transfer	Mass Flux	Concentration Gradient	Transfer Coefficient
(ft^3/min.)	(No./ft^3)	(No./min.)	(No/ft^3)	[No./min-ft^2 (No./ft^3)]
39.3	83-68-82	831.03	305	2.7247
	37-32-21	321.00	198	1.6212
	33-39-38	392.33	329	1.1925
	57-56-61	620.60	368	1.6864
	73-58-59	677.67	321	2.1111
	54-38-61	545.70	293	1.8625
	50-68-51	602.77	315	1.9135
28.7	25-28-29	653.20	271	2.4103
	28-35-25	624.80	257	2.4311
	23-28-29	568.00	216	2.6296
	41-39-34	809.40	311	2.6026
20	57-43-39	1390.00	356	3.9045
	39-41-41	1210.00	327	3.7003
	60-53-54	1670.00	375	4.4533
	67-70-76	2130.00	385	5.5325
10	58-62-50	2266.67	402	5.6385
	33-27-32	1226.67	265	4.6289
	38-37-47	1626.67	267	6.0924
	38-23-29	1200.00	243	4.9383
0	29-26-30	1416.67	291	4.8683
	41-43-53	2283.33	363	6.2903
	44-48-40	2200.00	456	4.8246
	48-59-61	2800.00	479	5.8455
-10	12-17-30	1179.99	168	4.6825
	43-40-37	2400.00	380	6.3158
	16-32-25	1279.99	162	5.2750

TABLE A-12.--Influence of air flow rate gradient on transport characteristics of air-borne bacteria with 0.5 ft^2 opening.

Air Flow Rate Difference (ft^3/min.)	Steady-State Transfer (No./ft^3)	Mass Flux (No./min.)	Concentration Gradient (No./ft^3)	Transfer Coefficient [No./min-ft^2 (No./ft^3)]
39.3	40-42-45	452.97	333	2.7205
	59-48-60	595.63	410	2.9055
	43-51-62	556.40	440	2.5291
28.7	19-32-20	540.10	197	5.1178
	17-40-28	603.50	268	4.5037
	56-38-50	1022.40	428	4.7776
	47-56-43	1036.60	447	4.6380
20	23-26-21	700.00	235	5.9575
	30-19-13	620.00	240	5.1667
	36-30-31	970.00	335	5.7910
	39-24-30	930.00	341	5.4546
10	34-37-43	1520.00	373	8.1501
	49-39-46	1786.67	376	9.5036
	19-20-32	946.67	207	9.1465
	25-30-27	1093.33	241	9.0733
0	42-45-39	2100.00	474	8.8607
	46-45-30	2016.60	433	9.3148
	52-29-17	1633.33	382	8.5515
	18-22-27	1116.67	242	9.2287
-10	21-21-19	1020.00	298	6.8456
	12-13-8	660.00	229	5.7642

TABLE A-13.--Influence of temperature gradient on the transport characteristics of air-borne bacteria at 61 ft^3/min.

Temperature Gradient (°F.)	Steady-State Transfer (No./ft^3)	Mass Flux (No./min)	Concentration Gradient (No./ft^3)	Transfer Coefficient [No./ft^2-min (No./ft^3)]
-14	16-13-17	935.33	272	2.2925
	20-13-14	955.67	252	2.4985
-12	24-21-20	1321.67	515	1.7109
	18-24-26	1382.67	433	2.1288
-11	28-27-33	1789.33	376	3.1726
	21-19-25	1321.67	350	2.5175
	18-17-20	1100.00	248	2.9569
	16-19-20	1100.00	257	2.8534
-10	41-34-43	2399.33	504	3.1737
	38-37-38	2297.67	473	3.2384
-6	48-39-56	2907.67	453	4.2791
	48-36-58	2887.33	404	4.7646
-5	40-43-41	2521.33	335	5.0176
	34-34-38	2155.33	341	4.2138
0	22-21-25	1382.67	189	4.8771
	22-27-24	1484.33	170	5.8209
	24-22-25	1443.67	154	6.2496
	54-50-44	3009.33	405	4.9536
5	29-27-29	1728.33	231	4.9880
	29-22-25	1545.33	215	4.7917
	19-25-15	1199.67	160	4.9986
	30-23-35	1789.33	162	7.3635
10	16-29-18	1281.00	149	5.7315
	21-29-19	1403.00	144	6.4954
	26-26-21	1484.33	173	6.5970
	25-20-24	1403.00	137	6.8273
12	28-30-19	1565.67	118	8.8455
	23-20-24	1362.33	117	7.7626
12.5	28-28-21	1423.33	121	7.8421
	17-25-27	1403.00	118	7.9266

TABLE A-14.--Turbulence data at various locations and flow conditions.

f (ft^3/min)	Location (in.)	$\overline{u'^2}$ (ft^2/min^2)	$\sqrt{\overline{u'^2}}$ (ft/min)	$\sqrt{\overline{u'^2}}/\bar{u}$ (%)
61-61	0	2.053	1.432	37.60
58-58	0	1.68	1.295	35.75
50-50	0	1.675	1.285	42.20
40-40	0	1.355	1.162	46.50
30-30	0	0.7503	0.866	46.15
20-20	0	0.419	0.646	48.60
50-20	8	0.025	0.158	11.89
50-20	6	0.0995	0.315	23.70
50-20	4	0.513	0.716	53.75
50-20	2	1.106	1.052	73.80
50-20	1	0.5069	0.711	41.70
50-20	0	0.7858	0.885	40.35
50-20	-1	1.343	1.159	43.10
50-20	-2	0.650	0.8055	27.20
50-20	-4	1.981	1.408	46.00
50-20	-6	1.277	1.128	36.85
20-20	-6	0.0041	0.064	4.81
20-20	-4	0.0096	0.0979	7.36
20-20	-2	0.112	0.3343	25.15
20-20	-1	0.164	0.4045	30.40
30-30	-4	0.503	0.710	37.75
30-20	8	0.2538	0.5035	26.82
40-40	8	0.4186	0.646	25.85
50-50	8	1.161	1.078	35.20
58-58	8	0.437	0.661	18.22
61-61	8	1.9994	1.412	37.03
20-60	8	1.415	1.189	31.68
50-70	0	1.479	1.215	32.65
50-60	0	2.538	1.59	46.65
40-70	0	1.647	1.282	37.30
30-70	0	2.8329	1.68	53.80
40-60	0	1.2095	1.099	35.18
30-60	0	1.942	1.393	49.60
40-50	0	0.675	0.821	29.20
20-50	0	1.4634	1.209	55.10
30-40	0	0.475	0.689	31.40
20-40	0	0.4334	0.6585	35.10
20-60	0	1.2057	1.098	43.90
30-50	0	1.0579	1.027	41.10
10-50	0	0.7823	0.884	47.15
10-40	-2	0.0587	0.2332	30.20
10-40	-6	0	0	0
10-40	0	0.6474	0.8035	50.75

TABLE A-15.--Dispersion data at various locations and flow conditions.

f	$\overline{u'^2}$	Integral	D_t	$\left(\overline{u'^2}\right)^{1/2}$	ℓ_1	t	$\overline{y^2}$	b
(ft^3/min)	(ft^2/min^2)	(min x 10^{-3})	(in^2/min)	(ft/min)	(in)	(min)	(in^2.)	(in.)
61-61	2.053	4.324	1.278	1.432	0.074	2.115	5.38	2.315
58-58	1.680	4.069	0.984	1.295	0.063	2.221	4.35	2.085
50-50	1.515	5.918	1.291	1.135	0.080	2.58	5.62	2.375
40-40	0.985	3.950	0.560	0.992	0.047	3.22	3.60	1.895
30-30	0.502	4.170	0.301	0.709	0.036	4.29	2.63	1.620
21.3-21.3	0.2115	3.467	0.106	0.459	0.019	6.05	1.27	1.126
50-70	2.091	2.306	0.694	1.443	0.040	1.84	2.55	1.596
50-60	1.5802	4.656	1.060	1.258	0.070	2.15	4.54	2.128
50-40	0.7848	2.922	0.330	0.864	0.030	3.22	2.00	1.414
50-30	0.7074	4.088	0.416	0.840	0.041	4.29	3.55	1.881
50-21.3	0.593	4.549	0.388	0.771	0.042	6.05	4.70	2.163
50-10.7	0.5805	3.267	0.273	0.761	0.030	12.04	6.60	2.565
40-70	1.7198	3.989	0.988	1.310	0.063	1.84	3.65	1.908
40-60	1.2090	3.301	0.575	1.098	0.044	2.15	2.49	1.577
40-50	0.7848	2.922	0.330	0.864	0.030	2.58	1.61	1.268
40-30	0.3644	4.534	0.238	0.603	0.033	4.29	2.05	1.431
40-21.3	0.2792	3.424	0.138	0.527	0.022	6.05	1.68	1.295
40-10.7	0.3237	4.510	0.210	0.568	0.031	12.04	5.09	2.252
30-70	1.6374	4.360	1.028	1.278	0.067	1.84	3.78	1.942
30-60	1.1266	5.705	0.926	1.060	0.073	2.15	3.99	1.996
30-50	0.7074	4.088	0.416	0.840	0.041	2.58	2.13	1.458
30-40	0.3644	4.534	0.238	0.603	0.033	3.22	1.54	1.240
30-21.3	0.3568	3.965	0.204	0.597	0.028	6.05	2.43	1.558
30-10.7	0.2115	4.925	0.150	0.459	0.027	12.04	3.58	1.890

REFERENCES

REFERENCES

Albertson, M. L., Dai, Y. B., Jensen, R. A. and Rouse, H.
1948 Diffusion of submerged jets. Proc. Am. Soc. Civil Engrs. 74:1571.

Batchelor, G. K.
1950 Note on free turbulent flows, with special reference to the two-dimensional wake. J. Aero. Sci. 17:441.

Batchelor, G. K.
1957 Diffusion in free turbulent shear flows. J. Fluid. Mech. 3:67.

Bourdillon, R. B., Lidwell, O. M. and Thomas, J. C.
1941 A slit sampler for collecting and counting air-borne bacteria. J. Hyg. 41:197.

Boussinesq, J.
1877 Essai sur la theorie des caux courantes. Memories presentes par divers savants a l'Academie des Sciences 23.

Cerna, M.
1961 Study of microbiological purity of air in dairies. Promysl. Protravin. 12:374.

Cheng, S. I. and Kovitz, A. A.
1958 Mixing and chemical reaction in the laminar wake of a flat plate. J. Fluid. Mech. 4:64.

Coles, D.
1956 The law of the wake in the turbulent boundary layer. J. Fluid. Mech. 1:191.

Corrsin, S.
1943 Investigation of flow in an axially symmetrical heated jet of air. NACA Wartime Report W-94.

Crank, J.
1956 The Mathematics of Diffusion. Clarendon Press, Oxford.

Csanady, G. T.
1963 On the energy balance of a turbulent mixing layer. J. Fluid. Mech. 15:545.

DallaValle, J. M.
1948 Micromeritics, the Technology of Fine Particles. Pitman Publishing Company.

Decker, H. M., Buchanan, L. M., Hall, L. B. and Goddard, K.R.
1962 Air Filtration of Microbial Particles. Public Health Service Publication No. 953. U. S. Government Printing Office, Washington, D. C.

DeOme, K. B. et al.
1944 The effect of temperature, humidity, and glycol vapor on the viability of air-borne bacteria. Am. J. Hyg. 40:239.

Druett, H. A. and May, K. R.
1952 A wind tunnel for study of air-borne infection. J. Hyg. 50:69.

Dryden, H. L. and Kuethe, A. M.
1930 Effect of turbulence in wind tunnel measurements. NACA Tech. Report No. 342.

Eckman, D. P.
1950 Industrial Instrumentation. John Wiley and Sons, Inc. New York.

Fage, A. and Falkner, V. M.
1932 Note on experiments on the temperature and velocity in the wake of a heated cylindrical obstacle. Proc. Roy. Soc. A135:678.

Flow Corporation.
1958 Model HWB2 hot wire anemometer theory and instruction, Flow Corp. Bulletin No. 37B.

Forstall, W., Jr. and Shapiro, A. H.
1950 Momentum and Mass Transfer in coaxial gas jets. J. Appl. Mech. 72:399.

Frenkiel, F. N.
1953 Turbulent Diffusion: Mean concentration distribution in a flow field of homogenious turbulence. Adv. Appl. Mech. 3:61.

Goldstein, S.
1930 Concerning some solutions of the boundary layer equation in hydrodynamics. Proc. Camb. Phil. Soc. 26:1.

Goldstein, S.
1933 On the two-dimensional steady-flow of a viscous fluid behind a solid body-I. Proc. Roy. Soc. London. A142:545.

Greene, V. W.
1965 Personal communication. School of Public Health. University of Minnesota. Aug. 10.

Hayakaw, I. and Poon, C. P.
1965 Short storage studies on the effect of temperature and relative humidity on the viability of air-borne bacteria. Ind. Hyg. J. 26:150.

Heldman, D. R., Hedrick, T. I., and Hall, C. W.
1964 Air-borne microorganism populations in food packaging areas. J. Milk & Food Tech. 27:245.

Heldman, D. R., Hedrick, T. I. and Hall, C. W.
1965 Sources of air-borne microorganisms in food processing areas-drains. J. Milk & Good Tech. 28:41.

Henderson, D. W.
1952 An apparatus for the study of air-borne infection. J. Hyg. 50:53.

Hinze, J. O., et al,
1948 Transfer of heat and matter in the turbulent mixing zone of an axially symmetrical jet. Appl. Sci. Res. A-1:435.

Hinze, J. O.
1959 Turbulence, An Introduction to its Mechanism and Theory. McGraw-Hill Co., Inc. New York.

Hollingdale, S. H.
1940 Stability and configuration of the wakes produced by solid bodies moving through fluids. Phil. Mag. 29 (7):209.

Howarth, L.
1934 Concerning the velocity and temperature distributions in plane and axilly symmetrical jets. Camb. Phil. Soc. Proc. 34:185.

Kalinske, A. A. and Pien, C. L.
1944 Eddy diffusion. Ind. Eng. Chem. 36:220.

Kaye, S.
1949 The sterilizing action of gaseous ethylene oxide. Am. J. Hyg. 50:290.

Kethley, T. W., Cown, W. B. and Fincher, E. L.
1956 A system for the evaluation of aerial disinfectants. Appl. Microbiol. 4:237.

Kethley, T. W., Cown, W. B. and Fincher, E. L.
1957 The nature and composition of experimental bacterial aerosols. Appl. Microbiol. 5:1.

Kuethe, A. M.
1935 Investigation of the turbulent mixing region formed by jets. J. Appl. Mech. Trans. ASME. 57:A87.

Labots, H.
1961 The estimation of the bacteria count of the atmosphere in dairy factories. Off. Org. K. Ned. Zuivelb. 53:772.

Laurell, G., Lofstrom, G., Magnusson, J.H. and Ouchterlony, O.
1949 Air-borne infection. 2. A report on methods. Acta Med. Scand. 134:189.

Leif, W. R. and Krueger, A. P.
1950 Studies on the experimental epidemiology of respiratory infections. J. Infectious Diseases. 87:103.

Leipmann, H. W. and Laufer, J.
1947 Investigation of free turbulent mixing. NACA TN 1257.

Lock, R. C.
1951 The velocity distribution in the laminar boundary layer between parallel streams. Quart. J. Mech. and Appl. Math. 4:42.

Mackay, I.
1952 Hexylresorcinol as an aerial disinfectant. J. Hyg. 50:82.

Olson, H. C. and Hammer, B. W.
1934 Numbers of microorganisms falling from the air in dairy plants. J. Dairy Sci. 17:613.

Pai, S. I.
1949 Two-dimensional jet mixing of a compressible fluid. J. Aero. Sci. 16:463.

Pai, S. I.
1954 Fluid Dynamics of Jets. D. Van Nostrand Company, New York.

Pai, S. I.
1955 On turbulent jet mixing of two gases at constant temperature. J. Appl. Mech. 22:41.

Pai, S. I.
1956 Laminar jet mixing of two compressible fluids with heat release. J. Aero. Sci. 23:1012.

Pasquill, F.
1962 Atmospheric Diffusion. D. Van Nostrand Company, Ltd. Princeton.

Porter, F. E., et al.
1963 The dynamic behavior of aerosols. Annals of the New York Academy of Sci. 105:45.

Prandtl, L.
1925 Berichte uber Untersuchungen zur ausgebildetan Turbulenz. ZAMM. 21:257.

Reichardt, H.
1941. Uber eine neue Theorie der freier Turbulenz. ZAMM. 21:257.

Reichardt, H.
1944 Impuls-und Warmeaustausch in freier Turbulenz. ZAMM. 24:268.

Rentschler, H. C.
1942 Bactericidal action of ultraviolet radiation on air-borne organisms. J. Bacteriol. 44:85.

Robertson, O. H., Puck, T. T. and Wise, H.
1946 The construction and operation of experimental rooms for the study of air-borne infection. J. Exptl. Med. 84:559.

Rosebury, T.
1947 Experimental Air-borne Infection. The Williams & Wilkins Company, Baltimore.

Schlichting, H.
1960 Boundary Layer Theory. McGraw-Hill Book Company, New York.

Sherwood, T. K. and Woertz, B. B.
1939 The role of eddy diffusion in mass transfer between phases. Trans. AI Ch. E. 35:517.

Silver, S. D.
1946 Constant flow gassing chambers: Principles influencing design and operation. J. Lab. Clin. Med. 31:1153.

Tanner, H. G.
1963 Evanescence of cloud chamber aerosols. Annals of the New York Academy of Sci. 105:27.

Taylor, G. I.
1915 Eddy motion in the atmosphere. Phil. Trans. Roy. Soc. A215:1.

Taylor, G. I.
1921 Diffusion by continuous movements. Proc. London Math. Soc. 20:(2):196.

Taylor, G. I.
1932 The transport of vorticity and heat through fluids in turbulent motion. Proc. Roy. Soc. A135:685.

Taylor, G. I.
1935 Statistical theory of turbulence. Part I. Proc. Roy. Soc. A151:444.

Tomotika, S.
1938 Application of the modified vorticity transport theory to the turbulent spreading of a jet of air. Proc. Roy. Soc. A165:65-72.

Torda, T. P., Ackermann, W. O. and Burnett, H. R.
1953 Symmetric turbulent mixing of two parallel streams. J. Appl. Mech. 20:63.

Towle, W. L. and Sherwood, T. K.
1939 Eddy diffusion: Mass transfer in the central portion of a turbulent air stream. Ind. Eng. Chem. 31:457.

Townsend, A. A.
1949 Momentum and energy diffusion in the turbulent wake of a cylinder. Proc. Roy. Soc. A197:124-140.

Townsend, A. A.
1956 The Structure of Turbulent Shear Flow. Cambridge University Press, New York.

Treybal, R. E.
1955 Mass Transfer Operations. McGraw-Hill Book Co., Inc., New York.

Twort, C. C., Baker, A. H., Finn, S. R. and Powell, E. O.
1940 The disinfection of closed atmospheres with germicidal aerosols. J. Hyg. 40:253.

Urban, E. C. J.
1954 Two chambers for use in exposing laboratory animals to inhalation of aerosols. Arch. Ind. Hyg. and Occupational Med. 9:62.

Webb, S. J.
1959 Factors affecting the viability of air-borne bacteria. I. Bacteria aerosolized from distilled water. Can. J. Microbiol. 5:649.

Weiss, E. and Stegeler, J. C.
1952 A cloud chamber for the uniform air-borne inoculation of mice. J. Infectious Diseases. 90:13.

Wells, W. F.
1933 Apparatus for study of the bacterial behavior of air. Am. J. Pub. Health. 23:58.

Wells, W. F.
1955 Air-borne Contagion and Air Hygiene. Harvard University Press, Cambridge.

Whitfield, W. J.
1963 Design of a dust controlled clean bench and hood utilizing laminar air flow. Presented at 2nd. Annual Convention of AACC. Boston, Mass. Apr. 30.

Wolf, H. W., Skaliy, P., Hall, L. B, Harris, M. M., Decker, H. M., Buchanan, L. M. and Dahlgren, C. M.
1959 Sampling Microbiological Aerosols. Pub. Health Rept. 74. U. S. Government Printing Office. Washington, D. C.

Wu, T. Y. T.
1962 A wake model for free-streamline flow theory-Part I. J. Fluid Mech. 13:161.